MODELING AND CONTROL OF BATTERY STORAGE SOLAR POWER GENERATION SYSTEM FOR ELECTRICAL REPLENISHMENT AT SEA FOR NAVAL SHIPS

A Project Report

submitted by

KUNAL MANI DOGRA

in partial fulfilment of the requirements
for the award of the degree of

MASTER OF TECHNOLOGY

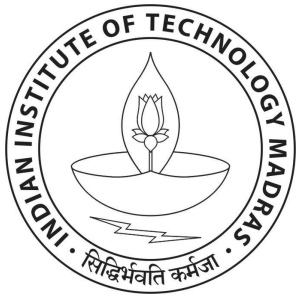

DEPARTMENT OF ELECTRICAL ENGINEERING
INDIAN INSTITUTE OF TECHNOLOGY MADRAS.

MAY 2017

THESIS CERTIFICATE

This is to certify that the thesis titled **Modeling and control of battery storage solar power generation system for electrical replenishment at sea for naval ships**, submitted by **KUNAL MANI DOGRA(EE15M008)**, to the Indian Institute of Technology, Madras, for the award of the degree of **Master of Technology**, is a bonafide record of the research work done by him under our supervision. The contents of this thesis, in full or in parts, have not been submitted to any other Institute or University for the award of any degree or diploma.

Dr Mahesh Kumar
Research Guide
Professor
Dept. of Electrical Engineering
IIT-Madras, 600 036

Place: Chennai

Date: May 2017

ACKNOWLEDGEMENTS

I would like to sincerely express my profound gratitude to my project guide, Dr Mahesh Kumar for his excellent guidance, motivation and constant support throughout the course of my project. His frequent interactions coupled with his patience have made this endeavour a success. I am also grateful for the laboratory facilities provided by him in the Power Quality and Automation Laboratory, ESB 354, Department of Electrical Engineering, which facilitated detailed simulation studies concerned to my work.

I greatly value and appreciate the encouragement by my fellow researchers and friends, who were always available as mentors and teachers in testing times. I cherish and retain fond memories of time spent in laboratory, learning research ethics and methodologies from my colleagues. In this context I would like to extend my gratitude towards my fellow mates Manik Pradhan, Srikanth Kotra, N Pruthvi Chaitanya, Leela Krishna Vedulla, Nafih Muhammad, Y Ram Shankar, A K Nitin Subramonium,T Sreekanth and my entire Mtech batch who were present to support and celebrate every effort and achievement of mine. I thoroughly enjoyed and cherish the discussions spanning over wide spectrum both related and non related to research, which helped me rejuvenate and keep interest in my work alive.

In the end a special word of thanks to acknowledge the support of my parents and my wife Natasha, who always stood by my decisions with unrelenting faith and were the source of inspiration for pursuing my endeavour. My heartfelt thanks to everyone who may have contributed to this endeavour, directly or indirectly.

ABSTRACT

KEYWORDS: Electrical replenishment at sea (ERAS);Perturb and Observe (P&O) ; Maximum Power Point Tracking(MPPT); charging current control; coupled inductor boost converter; super lift technique.

In an effort to safeguard India's trade routes extensive patrolling operations are undertaken by the navy. Naval ships or merchant vessels for that matter have been largely dependent on consumable fuel like coal and diesel for their operations. Complete elimination of the consumable fuel from onboard ships at present seems preposterous but supporting the existing set up with green fuel in order to limit the usage of former fuel is possible with existing advancement in the field of green fuel with solar being the most promising field.

The study proposes a model of a solar ship based on secondary data with its capability to generate enough power to cater for requirements of its sister ships during an operation or patrolling procedure. The existing capability of naval ships to synchronize to pass fuel could be harnessed to pass cable and transfer stored electricity. The solar ship is endeavored to harness solar energy using PV panels and store the energy in batteries for further utilisation, catering for twin purpose of meeting own ship load requirements and transferring the stored energy to sister ships during Electrical replenishment at sea (ERAS). Further, a simulation study with a sample data in Matlab/Simulink environment is undertaken to validate the proposed methodology under different modes of operation. With implementation of P& O MPPT algorithm, step reducing charging current control for battery charging and coupled inductor boost converter with super lift technique for battery discharging all possible day and night time scenarios for a naval ship are studied using the simulation and results are obtained.

Contents

List of Tables

List of Figures

Chapter 1

INTRODUCTION

1.1 Historical Importance of Shipping Industry

Indian sub continent with its tactical presence and fertile lands has been an attractive place for forces all over the world from time immemorial. In the contemporary scenario also, with home to one sixth of world's total population India is an attractive market for major workhouses around the world. In this context, trade, one of the oldest professions, has played a key role in establishing the stature of these lands over the centuries. Trade has been major contributor to expansion of human settlements and globalization. Further, if there had been trade, there have been seafarers, who dared the winds to present an economical means of transferring of materials and culture between civilizations over the sea. With established importance of sea going vessels for trade and in turn economy of the country, it was imperative, for navies all over the world, to safeguard all sea routes, critical for survival of the trade of their respective countries . Indian Navy in this context undertakes the job of protection of India's trade routes other than its role of safeguarding Indian shores from external aggression.

1.2 Fuel Usage in Shipping Industry

In an effort to safeguard India's trade routes extensive patrolling operations are undertaken by the navy, which brings forth the major cause of worry and need of the this study. Naval ships or merchant vessels for that matter have been largely dependent on consumable fuel like coal and diesel for their operations. The prime reason behind such extensive usage of these fuels is there reliability in terms of availability and operations. The operations onboard naval vessels starting from ship lighting, winch operations for boat lowering to mounting operation for weapons are of critical nature and of varied load profile. However, complete elimination of the consumable fuel from onboard ships at present seems preposterous but supporting the existing set up with green

fuel in order to limit the usage of former fuel is possible with existing advancement in the field of green fuel with solar being the most promising field. Shipping industry with its extensive usage of conventional fuel are major contributors in fast depletion of the existing stock of the conventional fuel and leader in green house gases emission due to combustion of such fuels. Emission from ships include oxides of nitrogen (NOx) which is a contributor in ozone formation, sulphur oxides (SOx), carbon dioxide, carbon monoxide and hydrocarbons. Fuel leakage at sea and harbour is another major cause of concern and threatens the ecosystem at sea. The introduction of green fuel in tandem with the conventional fuel onboard naval vessels thereby addresses some of the major issues which the world faces at present.

1.3 Horizon Enhancement with Green Fuel

The shipping industry comprises of two types of vessels those carrying cargo for commercial use called merchant ships and those undertaking patrolling operations called warships. The later are specific to a country and are responsible for safeguarding coastal borders of the country and ensuring safe passage of commercial ships from sea lines of communication (SLOC's). In order to undertake the second role the warships undertake extensive patrolling operations, which most of the times does not involve operation of pulse loads like weapon systems. Inclusion of renewable energy as power source onboard ships is underway in the commercial sector with merchant solar vessels like Auriga Leader with 328 solar panels being commissioned already, warships still await such feat. The major reason behind non inclusion of renewable energy on warships is the limited space availability on warships for solar panels and utilization of pulse loads on warships in times of operation. Electric power is essential to a modern naval ship's fighting and functional effectiveness. Electric power trains elevate gun turrets and missile launchers; operate the rudder, hydraulic system, run auxiliaries, provide light and power interior communication, weapons control, radio, radar, sonar and missile systems. A ship without electric power is useless as a fighting or supporting unit and is almost totally defenseless against enemy attack.

The study proposes a model of a solar ship based on secondary data with its capability to generate enough power to cater for requirements of its sister ships during an operation or patrolling procedure. At present navies around the world along with

Indian navy operates with oil tankers, which is a specialized class of ship capable of carrying large amount of conventional fuel. This fuel is transferred to other ships at sea during a procedure called RAS (Replenishment at sea) or UNREP. Underway replenishment (UNREP) operations to exchange fuel, food, parts or personnel are common in space, aerospace and marine operations. These rendezvous operations are essential in situations, where it is impractical to return to the base to replenish storage or personnel due to mission requirements. In particular, UNREP operations at sea are essential for long-term military operations to shorten or avoid port time [1]. UNREP sustains a Carrier Battle Group (CVBG) anywhere, anytime for as long as needed. A CVBG is normally deployed with 4-5 escort ships for a pre determined period. As part of CVBG, a replenishment ship (oil tanker ship) keeps the carrier and escorts stocked up with fuel. The evolution requires supplying ship to hold a steady course and speed. The receiving ship comes alongside the supplier at a distance of approximately 30 yards. Next, a gunline or a short line is fired using pneumatic line thrower from the supplier ship to the receiving ship, which is used to pull across a message line. This line is then used to pull across other equipments such as a distance line, phone line and fuel transfer rig lines. Once connected all further commands are directed from the supply ship. The procedure is elaborated in Fig.1.1 .

The existing capability of naval ships to synchronize to pass fuel could be har-

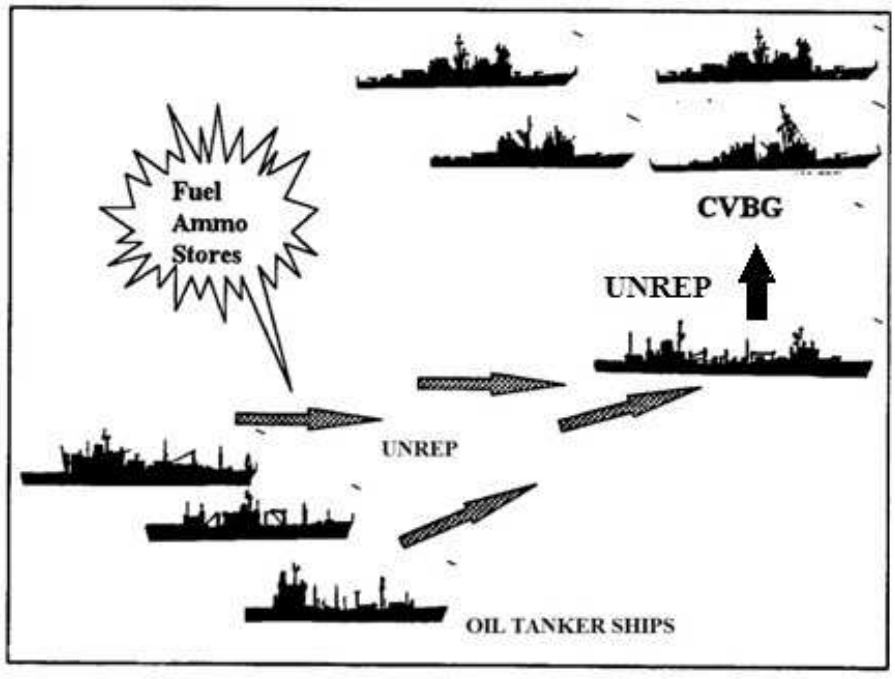

Fig. 1.1 UNREP at sea [1]

nessed to pass cable and transfer stored electricity. The solar ship is endeavored to harness solar energy using PV panels and store the energy in batteries for further utilisation, catering for twin purpose of meeting own ship load requirements and transferring the stored energy to sister ships during Electrical replenishment at sea (ERAS). The transferred energy from solar ship would be stored in a battery/ hybrid energy storage system at the target ship, as it would be addressed further in this work. The said work is directed to suggest/propose a methodology to increase the use of green fuel in the navy and reduce its dependence on the conventional fuel. The effort would help in countering the imminent global warming issue with reduction in emission of green house gases and on the operational front help the navy to increase longevity of its ships at sea with the same amount of fuel. It is an endeavor here to reduce the fuel consumption during patrolling and anchoring operation in particular as it is envisaged that during such operations pulse loads like missile systems are not utilized and the major load is the ship's lighting load, air conditioning system and navigation equipments.

1.4 Types of Non Conventional Fuel Sources

1.4.1 Wind Energy

The wind is a free, clean, and inexhaustible energy source. It has served mankind well for many centuries by propelling ships and driving wind turbines to grind grain and pump water. Interest in wind power lagged, however, when cheap and plentiful petroleum products became available after World War II. The high capital costs and the uncertainty of the wind placed wind power at an economic disadvantage. Wind power may become a major source of energy in spite of slightly higher costs than other conventional sources like coal or nuclear power because of the basically non-economic or political problems of coal and nuclear power. Presently, wind energy can be used from 800 kW to 6 MW of rated power.

1.4.2 Solar Power

Solar power systems are becoming more and more popular with increase of energy demand and concern of environmental pollution around the world. One of the inherent

advantages of PV generation is the absence of any mechanical parts. PV arrays are characterized by long service lifetime, exceeding 20 years, high reliability and low maintenance requirements and are suitable for remote area power supplies. In sunny locations, PV generators investment cost is comparable to wind generators in terms of PV modules per peak watt despite of higher investment cost of PV. Wind generators in comparison to PV generators require regular maintenance and are susceptible to damage to strong winds (a condition prevalent onboard naval vessels).

1.4.3 Small Hydropower

Amongst the alternate sources utilization of hydropower on a smaller scale (small, mini and micro hydropower) has become the thrust area for sustainable growth in the power sector. Hydropower is an economical and environmentally clean source of renewable energy abundantly available in hilly regions all around the world. Hydropower stations have an inherent ability for instantaneous starting, stopping, load variations, etc., and help in improving the reliability of power system. Hydropower energy generates power by using a dam or diversion structure to alter the natural flow of a river or other body of water. This energy can be used by conversion the water stored in dam into electrical energy using water turbines. There is huge hydropower potential in India which is located at inaccessible mountainous region. However, its development is challenging due to difficult and inaccessible terrain profile [3]. Hydroelectricity represents a large-scale alternative to fossil fuel generation and is a renewable and sustainable energy source to meet global challenges. Small hydro potential is available on small rivers, canal heads and canal drops. Of all the nonconventional renewable energy sources, small hydropower represents highest density resource and stands in first place in the generation of electricity from renewable sources throughout the world. Global installed capacity of Small Hydropower today is around 47,000 MW against an estimated potential of 180,000 MW [3].

1.5 Suitability of Solar Energy for Naval Scenario

A major reason that has made harvesting and utilization of solar energy possible is its profuse availability. Solar energy can be a standalone producing system or can

be a grid connected generating unit depending on the availability of a grid nearby. In naval scenario, a ship can be seen as a microgrid system with diesel generators forming the heart of the electrical design and their correct sizing is key to safe, workable and economical system. SOLAS- international maritime regulations require at least two generators for ship's main electrical power system to cater for generator's susceptibility to large system load swings, loads causing distortion, the connection of motors and connection of large heater elements of air conditioning systems. Rising cost of fuel and the necessity to reduce emissions of pollutant gases have led to an increased focus on development of renewable energy sources in ship industry. Ships are one of the main producers of greenhouse gases and responsible for 3 % of global carbon dioxide emissions per year. Therefore, use of renewable energy resources in power system of ships would be a great advantage, particularly in reducing carbon dioxide emissions and gaining independence on highly unpredictable fuel price. MARPOL 73/78, one of the most important international marine environmental conventions has included Energy Efficiency Design Index (EEDI) and Ship Energy Efficiency Management Plan (SEEMP) in 2011 [4].

Solar energy is one of the most applicable sources for marine use due to its abundant availability and absence of obstructing structures at sea making harnessing of solar energy to full capacity possible at sea. According to a study, solar panels were observed to produce 1.4 times more energy on the ship at sea than on land in Tokyo [4]. It is suggested that being at sea means more sunlight and also the wind encountered cools off the panels and thereby increasing the efficiency. Solar ship in this regard integrates solar PV system into the ship power system. Core concept of solar ship is to reduce the fuel consumption and gas emission of traditional diesel generator by applying the PV power. Load power requirement can even be satisfied by the power source of PV system only, so DG is set as a standby electric power unit during navigation thereby eliminating gas emission. DG is put into use only in special situation e.g., rainy weather or PV system failure [4].

1.6 Research Motivation

Rising cost of fuel and the necessity to reduce emissions of pollutant gases from the shipping industry are few of the major motivating factors for undertaking the pro-

posed study. Therefore, use of solar energy in power system of ships would be a great advantage, particularly in reducing carbon dioxide emissions and gaining independence on highly unpredictable fuel price. The effort would help in countering the imminent global warming issue with reduction in emission of green house gases and would also prove to be helpful to the navy to increase longevity of its ships at sea with the same amount of fuel. It is an endeavor here to reduce the fuel consumption during patrolling and anchoring operation in particular as it is envisaged that during such operations pulse loads like missile systems are not utilized and the major load is the ship's lighting load, air conditioning system and navigation equipments which are believed to be catered by PV system easily

1.7 Objectives of Study

As brought out in the earlier sections the area of research involves inclusion of renewable sources of energy with the ship power systems, thereby requires a blend of study on MPPT control strategies to harness maximum power from solar panels using DC-DC converters, dc bus regulation schemes, charging/ discharging control for the batteries acting as energy storage devices and control scheme for charging target ship batteries utilizing the energy harnessed using solar panels. Based on the above facts, the objectives are formulated as:

- Collection of load data from fleet ships so as to analyze the required power to be harnessed from solar panels to smoothly run the existing setup.
- Based on the collected secondary data, propose size of a solar ship that would suffice the need of the fleet ships, thereby undertaking a feasibility study for the proposed methodology.
- To simulate the proposed topology and algorithm in MATLAB/SIMULINK to validate the proposed ideas.

1.8 Organisation of Thesis

The thesis is divided into **six** chapters bringing out the theoretical concepts on which the study is based.

Chapter 1 brings out the suitability of the study in the present scenario, thereby stating the existing practices of the shipping the industry and relevance of introduction of solar energy of all the renewable energy sources to the naval scenario. Further, the chapter provides the motivation behind the research and its objectives.

Chapter 2 discusses about the feasibility of fitment of solar panels on the existing ships of the naval fleet based on the loading data collected for different states of operation of a naval ship. The study suggests a suitable size of a solar ship for catering all non critical loads or loads not affecting war fighting capability of the ship, using renewable energy. Also, the chapter introduces solar panels and its implementation in Matlab/Simulink environment.

Chapter 3 discusses the theory behind Maximum Power Point tracking and different ways of its implementation. Further, the chapter also brings out Matlab/Simulink implementation of MPPT using boost converter and its importance in the present study.

Chapter 4 discusses different battery charging techniques and the implementation of battery charging using stepped reduction in current for the present study. Also, battery discharging circuit utilizing coupled inductor boost converter with super lift techniques is discussed in detail to bring out its working and Matlab/Simulink implementation.

Chapter 5 discusses different cases of operation of the proposed methodology elaborately, charting out the circuitry involved in each of the cases. Further, results obtained from the simulation study in Matlab/Simulink environment are provided in the chapter to verify the proposed ideas of the study.

Chapter 6 presents important conclusions of the present study. Also, suggestions are provided for future scope of work.

Chapter 2

FEASIBILITY STUDY FOR DESIGN OF SOLAR SHIP AND MODELLING OF PV MODULE

2.1 Introduction

The present study endeavours to propose a methodology to introduce green fuel to the existing set up of the navy. The navy operates with a variety of ships, together comprising of a naval fleet. Each of the ship as part of a naval fleet, specialises in a specific aspect of naval operations. Individually, each vessel of a naval fleet is a critical component and enabler for proper discharge of duties by the fleet. Some ships like aircraft carriers, missile corvettes and destroyers constitute the front line of defence, whereas ships like oil tankers assumes the most important logistics support role. The feasibility study as described in this chapter firstly analyses the existing ships for availability of adequate unobstructed area for fitment of solar panels. The aim of the study was to ascertain, if the ships can harness enough solar energy individually to meet its load requirements. However, it is observed that a naval warship is fit with number of operational and tactical equipments on the upper deck and has very less free space to offer. Thereby, in order to proceed with the study, it was essential to decide upon a appropriate size of solar ship, to be a part of naval fleet, for catering the load of fleet ships. Towards this, the feasibility study is subsequently described based on load data obtained from naval fleet.

2.2 Feasibility Study for Design of Solar Ship

Study of load requirements of a naval ship can be classified under following three heads which bring about the state of operation of the ship and gives an insight into type of equipments under utilization.

Table 2.1: Load profile for different type of ships

S.No.	Ship Type	Harbour (kW)	Cruising (kW)	Action (kW)
1	Guided missile destroyer	490	1150	1350
2	Anti submarine warfare ship	490	847	1769
3	Amphibious vessel	240	372	503
4	Guided missile corvette	205	407	565
5	Minesweeper	100	150	190

- **Harbour load**: When at harbour all navigation equipments, pulse loads like weapon load etc. are off and the major load of the ship comprise of lighting and air conditioning load.
- **Cruising load**: This load value brings forth the ship loading at sea i.e., during sailing wherein ship is undertaking patrolling exercise. In this case in addition to the harbour load, navigation equipments are switched on. However, weapon machinery is off for this condition.
- **Action load**: This condition depicts war scenario/ war exercises and requires maximum machinery onboard ship to be switched on. The ship borne generators are under maximum loading in this condition. In addition to the cruising load the action loading involves switching on off all or required weapon equipment based on the exercise undertaken at sea.

The data collected from a naval fleet for undertaking a feasibility study for installation of solar panels on the existing ships is given in Table 2.1 Given the critical nature of certain loads onboard naval vessels, complete removal and replacement of existing diesel generators is a preposterous task, however, supplementing the existing set up to take over non critical loads is the endeavor of this study. Towards this, it is observed that harbour load which primarily includes lighting supply, air conditioning, sewage treatment plants etc are the non critical load which do not directly affect the war fighting capability of a naval warship. Therefore, limiting the scope of study to the harbour load data, further existing ships are analyzed for space availability for fitting of solar panels.

Considering solar panel SUNPOWER X-21, 345 as basic component for undertaking this study and a sample load data is given in Table 2.2. Size of solar panel SUNPOWER X-21, 345 as per manufacturer data sheet is given as

$$Area\ of\ panel = 1.76\ m^2. \tag{2.1}$$

Covered area required to cater for 2500 kW from above solar panels considering 6.5 hrs

Table 2.2: Sample Load data of naval ship

S.No.	Harbour (kW)	Cruising (kW)	Action (kW)
Per hour load			
1	50	75	100
Full day requirement (24 hrs)			
2	1200	1800	2400

of daily sunlight is given as

$$Required\ covered\ area = \frac{2500 * 1.76}{345 * 6.5} \ = \ 2100\ m^2. \tag{2.2}$$

Further, considering 30% of available area as walking rows between panels, we have

$$Z - 0.3Z = 2100\ m^2. \tag{2.3}$$

Therefore,

$$Z = 3000\ m^2. \tag{2.4}$$

Where,
Z = Required covered area in m^2.

The outcome of the above study suggests the suitability of a separate solar ship for meeting the requirement instead of putting up individual solar panels on existing warfare ships. This owes to the fact that all warships are cluster of varied war fighting equipments which includes radars, weapons, navigation equipments etc. which are placed at the upper deck of the ship, thereby limiting the available free space for allowing solar panel fitment. Besides, nature of activities undertaken by the naval ships require them to allow free movement of personnel on the upper deck. Therefore, based on the value of required covered area as calculated above for the sample ship data certain combinations of deck length and width giving an area of 3000 m^2 are possible. A ship of length 150 m and 20 m width is considered suitable owing to its close resemblance to sizes of existing naval oil tanker ship sizes. However, the solar ship of the proposed size would be capable for catering of action load of the sample ship but would

Table 2.3: Load data for simulation study

S.No.	Harbour (kW)	Cruising (kW)	Action (kW)
Per hour load			
1	2	3	4

not be able to support its own machinery. Therefore, considering a ship of dimension of 250 m length and 30 m width, following is calculated

$$Available\ area\ =\ 250 * 30\ =\ 7500\, m^2. \tag{2.5}$$

Considering 30% of total area for walking rows

$$Area\ consideration\ for\ walking\ rows\ =\ 0.3 * 7500\ =\ 2250\, m^2. \tag{2.6}$$

Therefore,

$$Net\ available\ area\ =\ 7500\ -\ 2250\ =\ 5250\, m^2. \tag{2.7}$$

Further,considering six sections of the ship,

$$Net\ area\ per\ section\ = \frac{5250}{6}\ =\ 875\, m^2. \tag{2.8}$$

Therefore,

$$Number\ of\ panels\ per\ section\ =\ \frac{875}{1.76}\ =\ 497\ units \tag{2.9}$$

and

$$Power\ output\ of\ solar\ panels\ per\ section\ =\ 345 * 6.5 * 497\ =\ 1114.5\, kW. \tag{2.10}$$

From the above results it is evident that a solar ship of the proposed dimension can cater for the load of the sample ship alongwith its own load. However, to maintain fast mobility which is critical for a naval platform, multiple solar platforms/ships in a fleet of smaller sizes would be ideal for optimizing between operational and tactical requirements. Further, for simulation study of the proposed methodology the sample ship load requirement is scaled down to 25 times, as brought out in Table 2.3.

2.3 Modelling of PV Module

Among the non conventional sources of energy photovoltaic (PV) source or solar energy is the most sustainable source of energy owing to its ubiquity and abundant nature. Regardless of intermittent nature of sunlight solar energy is widely available and free of cost. PV module with its combination of PV cells generates DC current when exposed to direct sunlight without environmental contamination. PV module thereby, is the fundamental power conversion unit of a PV generation system. The output characteristic of PV module depends on solar insolation, cell temperature and output voltage of PV module [5]. The typical I-V curves of PV module are shown in Fig. 2.3. It is observed that when load is connected to panel, it changes the value of voltage and current.

The electromagnetic radiation of solar energy can be directly converted to electricity through photovoltaic effect. When exposed to the sunlight, photons with energy greater than the band gap energy of the semiconductor are absorbed. Absorption of the incident photon result in creation of electron hole pairs proportional to incident radiation. Further, under the influence of internal electric fields of the p-n junction, the generated carriers are swept apart and hence a photocurrent is generated [6].

2.3.1 Solar cell model

A general model of solar cell consist of a photocurrent source, a diode, a parallel resistor expressing a leakage current and a series resistor describing an internal resistance to the current flow as shown in Fig. 2.1. The voltage current characteristic

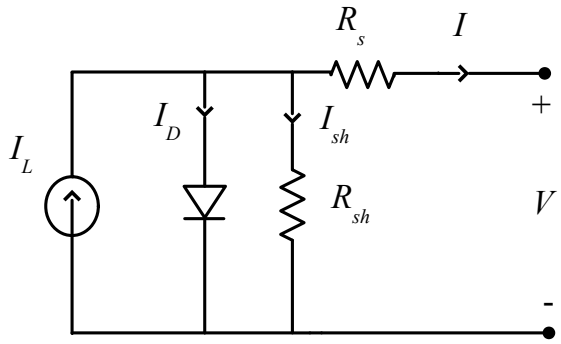

Fig. 2.1 Solar cell single diode model

equation of a solar cell is given as in (2.11) (by using KCL),

$$I = I_L - I_D - \frac{(V + IR_S)}{R_{SH}} \tag{2.11}$$

where,

I_L- light generated current or photocurrent

I_D-diode current

R_S- series resistance

R_{SH}- shunt resistance.

Further, according to Shockley diode equation in (2.12)

$$I_D = I_S[exp\frac{q(V + IR_S)}{kT_CA} - 1] \tag{2.12}$$

where,

I_S- diode leakage current density in absence of light

q- electron charge = $1.6 * 10^{-19}\ C$

k- boltzmann's constant = $1.38 * 10^{-23}\ J/K$

T_C- Cell's working temperature

A- Ideal factor

Substituting (2.12) in (2.11)

$$I = I_L - I_S[exp\frac{q(V + IR_S)}{kT_CA} - 1] - \frac{(V + IR_S)}{R_{SH}} \tag{2.13}$$

The photocurrent in the above equation in turn depends on solar insolation and cell's working temperature, which is described as

$$I_L = [I_{SC} + K_I(T_C - T_{Ref})]\frac{\varphi}{\varphi_{Ref}}. \tag{2.14}$$

Where,

I_{SC}- Cell's short circuit current at 25^oC and $1\ kW/m^2$

K_I- Cell's short circuit temperature coefficient

T_{Ref}- Cell's reference temperature

φ- Solar radiation

φ_{Ref}- Reference solar radiation $(1000\ W/m^2)$.
Also, the diode leakage current density I_S in (2.12) can be further defined as follows

$$I_S = I_{RS}(\frac{T_C}{T_{Ref}})^3 exp\frac{qE_G(\frac{1}{T_{Ref}} - \frac{1}{T_C})}{kA}. \tag{2.15}$$

Where,
I_{RS}- Cell's reverse saturation current at a reference temperature and a solar radiation.
E_G- Band gap energy of semiconductor used in the cell

Now, in order to obtain a simplified PV solar cell model it is observed that the shunt resistance R_{SH} is inversely related to shunt leakage current to ground, therefore PV efficiency is insensitive to variation in R_{SH} and the shunt leakage resistance can be assumed to approach infinity. On the other hand, a small variation in series resistance R_S will significantly affect the PV output power. Thereby, modified model of PV solar cell can be rewritten as in (2.16),

$$I = I_L - I_S[exp\frac{q(V + IR_S)}{kT_CA} - 1]. \tag{2.16}$$

Further, considering an ideal PV cell, there is no series loss and no leakage to ground, i.e $R_S = 0$ and$R_SH = \infty$. Then, the above equivalent circuit of PV cell can be rewritten as following [7],

$$I = I_L - I_S[exp\frac{qV}{kT_CA} - 1]]. \tag{2.17}$$

2.3.2 PV Module

A typical solar cell produces less than 2 W at 0.5 V approximately. Therefore, in order to achieve higher output power solar cells are connected in series and parallel configurations on a module. A PV array is a group of several PV modules connected in series and parallel to generate required current and voltage. Subsequently, modified equation for solar array is as brought out in 2.18 [8],

$$I = N_PI_L - N_PI_S[exp\frac{q(\frac{V}{N_S} + \frac{IR_S}{N_P})}{kT_CA} - 1] - (\frac{(\frac{N_PV}{N_S} + IR_S)}{R_SH}). \tag{2.18}$$

Where,

N_P - number of cells connected in parallel

N_S - number of cells connected in series

Commercially PV cells are connected in series configuration to form a PV module with adequate working voltage. These PV modules are further arranged in series-parallel structure to achieve desired power output.

2.4 Simulation of PV Module (MATLAB/SIMULINK)

In order to meet requirement of the project, a series-parallel combination of solar panel module of the make SUNPOWER X-21, 345 was implemented in MATLAB/SIMULINK environment. Parameters as per the manufacturer's data sheet of the simulated panel are as shown in Table 2.4 . 4 kW of power was determined to be the desired power output from the array. The simulation of the PV array was implemented with the help of MATLAB function as shown in Fig. 2.2 . The implementation involves combination of 576 cells (96x6) in series (i.e. six panels in series) forming one module and further two such modules connected in parallel to achieve required power output of 4 kW. Fig.2.3 gives the typical current-voltage (I-V) characteristics of a PV module correspondingly for different irradiation values. It is observed that maximum current values for a PV module decreases with decreasing irradiation values. Also, P-V characteristic curves for simulated module with changing irradiation levels as shown in Fig. 2.4 depicts that maximum power output from the PV module decreases as there is decrease in irradiation levels. It is seen that the output characteristics of the solar module is nonlinear and extremely pretentious by the solar irradiation, temperature and load change. To maximize power from solar module, it has to be worked at fixed value of voltage and current which is defined by manufacture, or at a definite value of load resistance. This needs DC-DC converter circuit to track maximum power from PV module or panel work at a fixed value of voltage and current. In this project, a boost type DC-DC converter is used to extract the maximum power from solar module by matching load to the PV module.

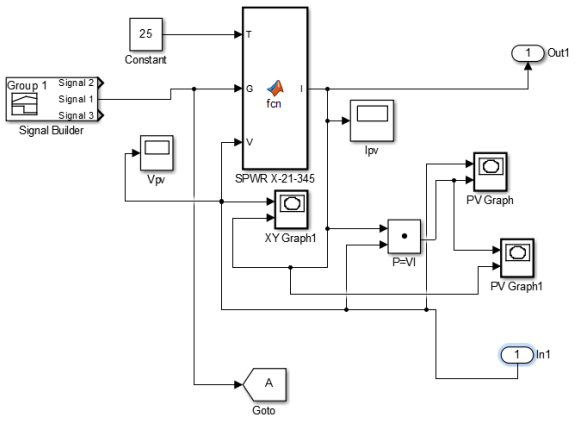

Fig. 2.2 Subsystem implementation of generalised PV model

Table 2.4: Manufacturer's data for SUNPOWER X-21 345 solar panel

SUNPOWER X-21 345		
S.No.	Parameter	Value
1	STC Power rating	345W
2	PTC Power rating	323.3 W
3	Temp coeff of Isc	0.05%/K
4	Temp coeff of Power	-0.3%/K
5	Temp coeff of Voltage	-0.164V/K
6	Number of cells	96
7	Imp	6.02A
8	Vmp	57.3V
9	Isc	6.39A
10	Voc	68.2V

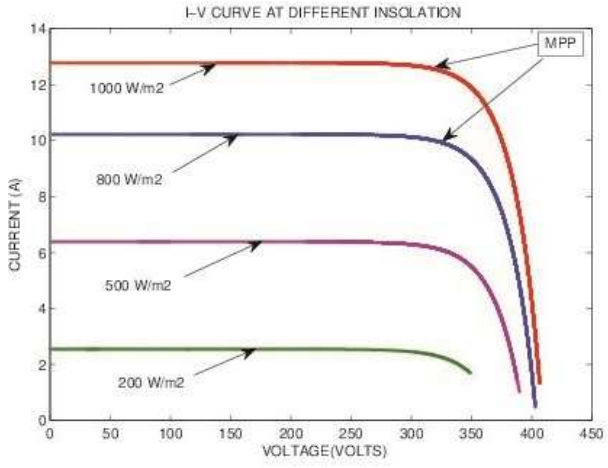

Fig. 2.3 I-V curve for PV panel

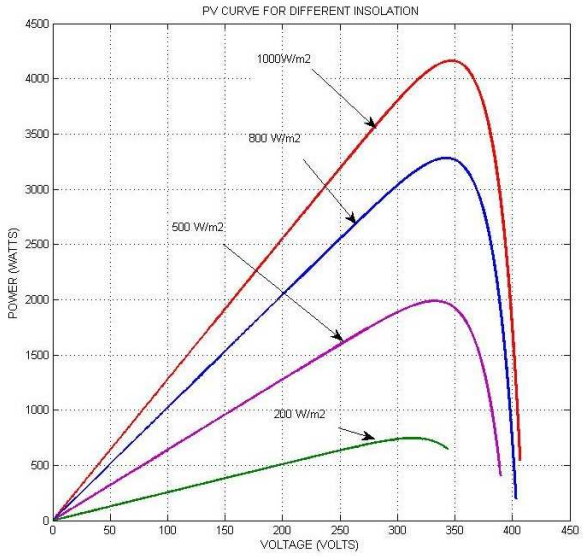

Fig. 2.4 P-V curve for solar panel at different insolation values

2.5 Conclusion

The chapter discusses about the feasibility of fitment of solar panels on the existing ships of the naval fleet. The discussion was based on the loading data collected for different states of operation of a naval ship. The study was directed to suggest a suitable size of a solar ship for catering all non critical loads or loads not affecting war fighting capability of the ship, using renewable energy. Further, the chapter discusses the theory behind mathematical modeling of solar panels and its implementation in Matlab/Simulink environment.

Chapter 3

MAXIMUM POWER POINT TRACKING TECHNIQUES

3.1 Types of MPPT Algorithms

Maximum power point (MPP) describes the point on a PV current voltage (I-V) curve at which the solar PV device generates the largest output i.e where the product of current intensity and voltage is the maximum. The MPP may change due to external factors such as temperature, light conditions and workmanship of the device. The Maximum Power Transfer theorem states that the power output of a circuit is the maximum when Thevenin impedance of a circuit matches with the load impedance. Accordingly, Maximum power point tracking is a load matching problem and involves matching/ changing the input resistance of the panel to match the load resistance. Studies show that a solar panel converts 30-40 % of energy incident on it to electrical energy. Therefore, implementation of MPPT algorithm is essential to increase the efficiency of the system.

In the source side a boost convertor is connected to the solar panel in order to enhance the output voltage so that it can be used for different applications like motor load. Thereby, by an appropriate change in the duty cycle of the boost converter, source impedance can be made to match the load impedance, hence achieving the application of MPPT (Maximum Power Point Tracking Algorithm). There are different techniques used to track the maximum power point as follows

- Perturb and observe (hill climbing method)
- Incremental conductance method
- Fractional short circuit method
- Fractional open circuit voltage
- Neural network
- Fuzzy logic.

The choice of the algorithm depends on the complexity, time algorithm takes to track the MPP, implementation cost and the ease of implementation.

3.1.1 Perturb and Observe

Perturb and Observe (P & O) is the simplest method for MPPT implementation. Both P & O and incremental conductance algorithms are based on the "hill-climbing" principle, which consists of moving the operation point of the PV array in the direction in which power increases. It utilizes only one sensor, that is the voltage sensor, to sense the PV array voltage and so the cost of implementation is less and hence easy to implement. In this method, the sign of the last perturbation and the sign of the last increment in the power are used to decide what the next perturbation should be. If there is an increment in the power, the perturbation should be kept in the same direction and if the power decreases, then the next perturbation should be in the opposite direction. Based on these facts, the algorithm is implemented [9]. The process is repeated until the MPP is reached. The time complexity of this algorithm is very less but on reaching very close to the MPP the algorithm does not stop at the MPP and keeps on perturbing on both the directions. When this happens, the algorithm has reached very close to the MPP and an appropriate error limit can be set or a wait function can be used which ends up increasing the time complexity of the algorithm. However, the method does not take account of the rapid change of irradiation level (due to which MPP changes) and considers it as a change in MPP due to perturbation and ends up calculating the wrong MPP. To avoid this problem incremental conductance method can be used. Flowchart for the above algorithm is given in Fig. 3.1

3.1.2 Incremental Conductance

Incremental conductance method uses two voltage and current sensors to sense the output voltage and current of the PV array. The incremental conductance algorithm is based on the fact that the slope of the curve power vs. voltage (current) of the PV module is zero at the MPP, positive (negative) on the left of it and negative (positive) on

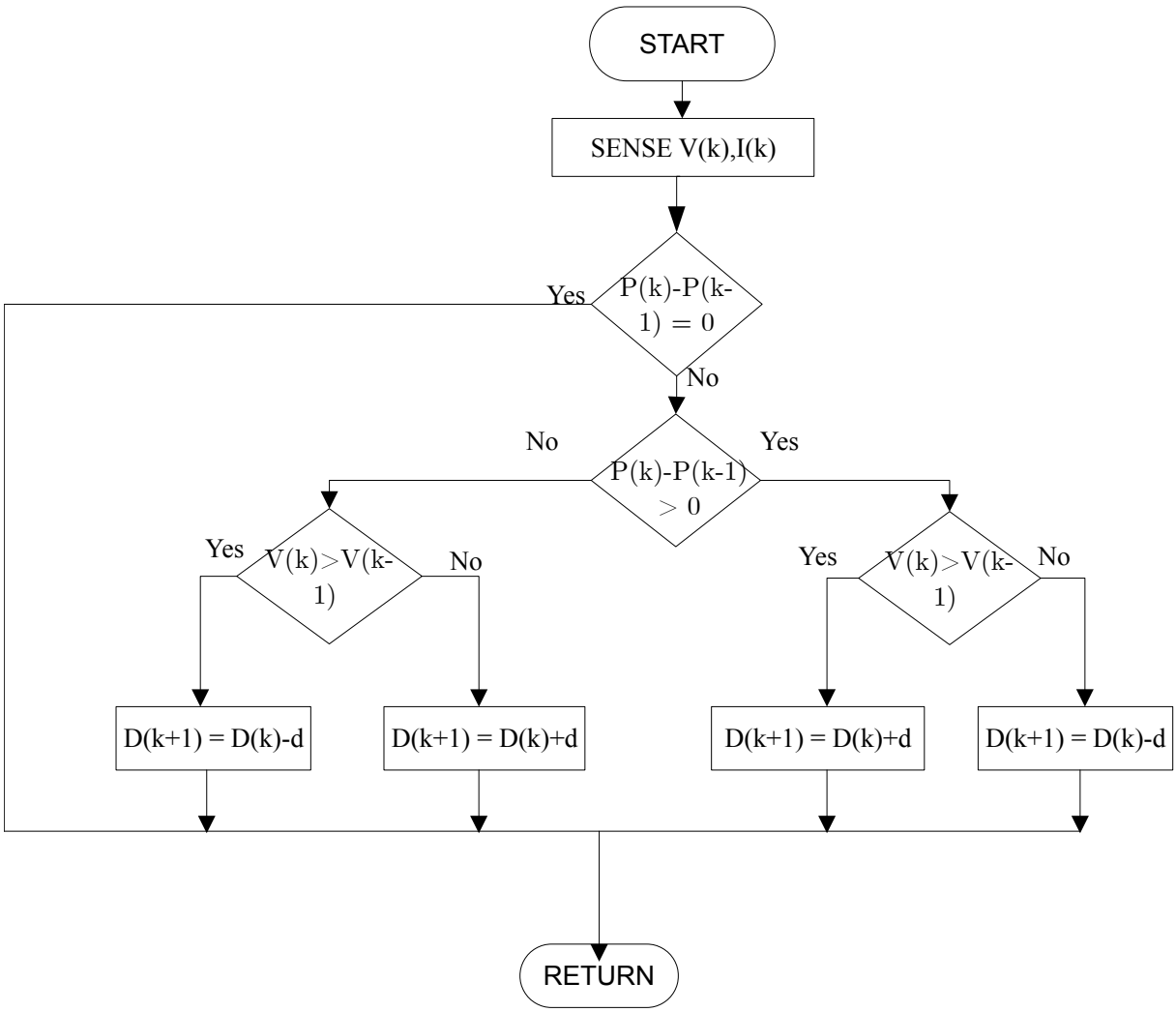

Fig. 3.1 Perturb and Observe MPPT algorithm

the right, i.e., at MPP [10].

$$\Delta V/\Delta P = 0(\Delta I/\Delta P = 0) \tag{3.1}$$

whereas, on the left of MPP

$$\Delta V/\Delta P > 0(\Delta I/\Delta P < 0) \tag{3.2}$$

And, on the right of MPP

$$\Delta V/\Delta P < 0(\Delta I/\Delta P > 0) \tag{3.3}$$

The algorithm utilizes incremental conductance (dI/dV) of the photovoltaic array to calculate the sign of the change in power with respect to voltage (dP/dV).

$$P = V * I \tag{3.4}$$

$$dP/dV = I + V * dI/dV \tag{3.5}$$

At MPP point

$$I + V * dI/dV = 0 \tag{3.6}$$

whereas, on the left of MPP

$$I + V * dI/dV > 0 \tag{3.7}$$

And, on the right of MPP

$$I + V * dI/dV < 0 \tag{3.8}$$

In this case both the voltage and current are sensed simultaneously. Therefore, the error due to change in irradiance prevalent with perturb and observe algorithm is eliminated. However, the complexity and the cost of implementation increase. Flowchart elaborating the above algorithm is given in Fig. 3.2.

3.1.3 Fractional Open Circuit Voltage

This method uses the approximately linear relationship between the MPP voltage (Vmpp) and the open circuit voltage (V_{oc}), which varies with the irradiance and temperature [11].

$$V_{mpp} \approx k * V_{oc} \tag{3.9}$$

Where, k is a constant depending on the characteristics of the PV array which is required to be determined beforehand by determining the V_{mpp} and V_{oc} for different levels of irradiation and different temperatures. k has been reported in literature to be between 0.71 and 0.78. Further, V_{mpp} can be determined by measuring V_{oc} periodically. In order to measure V_{oc} the power converter has to be shut down momentarily. Therefore, in each measurement there is a power loss. Another problem of this method is that it

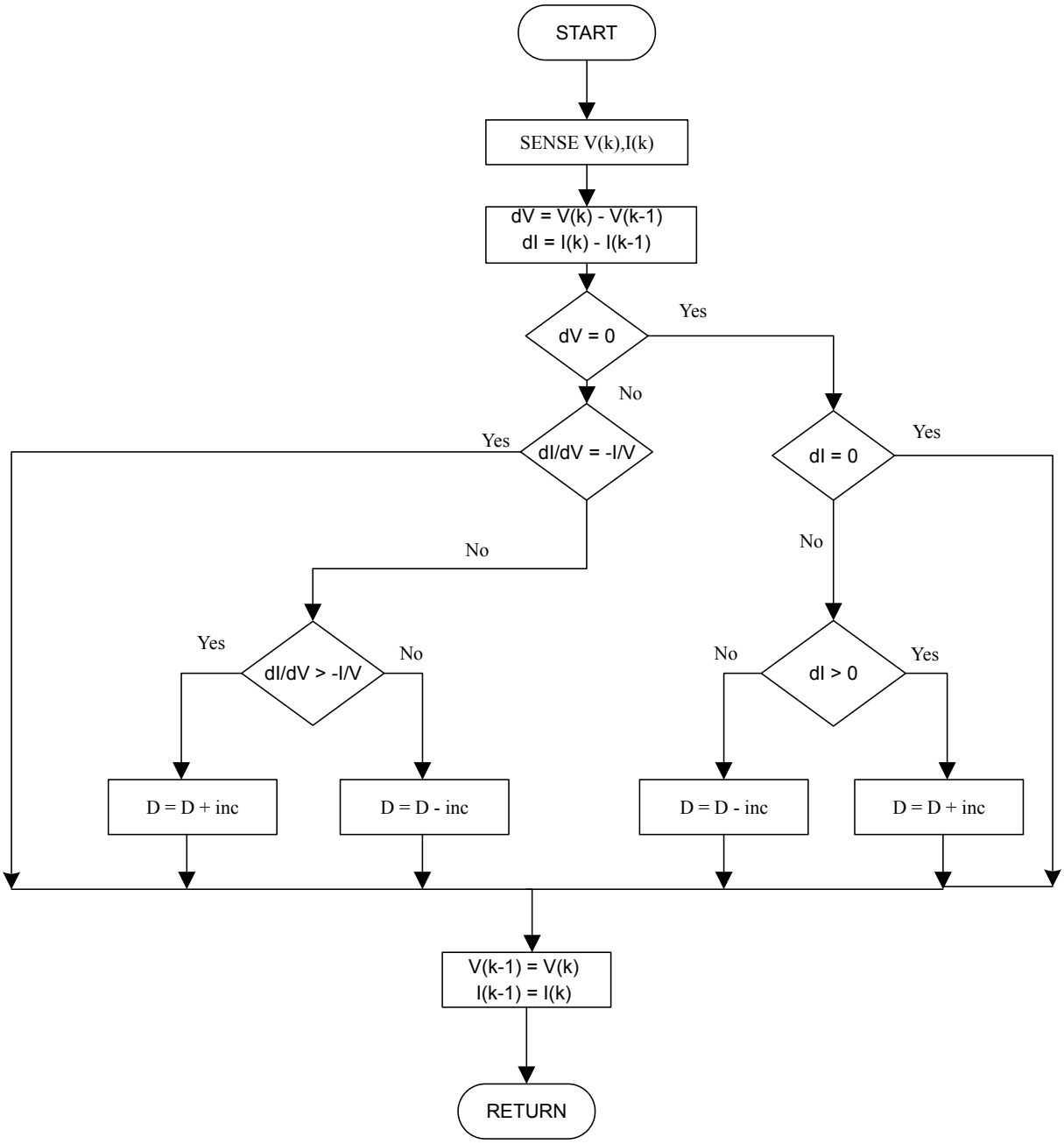

Fig. 3.2 Incremental conductance MPPT algorithm

is incapable of tracking the MPP under irradiation slopes, because the determination of V_{mpp} is not continuous. One more disadvantage is that the MPP reached is not the real one because the relationship is only an approximation. The technique can be used depending on the application as it is easy and cheap to implement. It does not require DSP or micro-controller control and just one voltage sensor is used. However, this method is not valid under partial shading of the PV array as under this condition k changes. To update k a voltage sweep is proposed though this increases the complexity of the system, the cost increases and there are more power losses during the sweep [12].

3.1.4 Fractional Short Circuit Current Method

Similar to the fractional open circuit voltage method, there exists an approximate relationship, between the short circuit current I_{sc} and the MPP current, I_{mpp}, as is shown by

$$I_{mpp} \approx k_1 * I_{sc}. \tag{3.10}$$

The coefficient of proportionality k_1 is required to be determined according to each PV array. Measurement of the short circuit current while the system is operating is difficult. Therefore, it usually requires adding an additional switch to the power converter to periodically short the PV array and measure I_{SC}. In [13], I_{SC} is measured by shorting the PV array with an additional field-effect transistor added between the PV array and the DC link capacitor. Besides, a boost converter is used to short the PV array in [14]. Short circuiting the PV array also leads to a loss of power. Similar to the fractional open circuit voltage method, the real MPP is not reached because the proportional relationship is an approximation. Furthermore, k_1 changes if the PV array is partially shaded, which happens due to shades or surface contamination.

3.1.5 Fuzzy Logic Control

A fuzzy controller is a technique to embody human like thinking into the control system. It is designed to emulate human deductive thinking, i.e., deriving conclusion utilizing prior known knowledge. Fuzzy logic is a mathematical system that analyzes analog input values in terms of logical values that can take continuous values from 0 to 1, unlike digital controller that can take values of either 0 or 1. The fuzzy logic consists of three stages: fuzzification, inference system (application of fuzzy rules) and defuzzification (obtaining the crisp or actual results). Fuzzification comprises the process of transforming numerical crisp inputs i.e., well defined inputs, into linguistic variables based on the degree of membership to certain sets. This step is utilized to graphically define a function. Membership functions are used to associate a grade to each linguistic term. The number of membership functions used depends on the accuracy of the controller, but it usually varies between 5 and 7 [15, 16, 17]. The inputs of the fuzzy controller are usually an error, E, and the change in the error, ΔE. The error can be chosen by the designer, but usually it is chosen as $\Delta P/\Delta V$ because it is zero at the

MPP.

$$E = (P(k) - P(k-1))/(V(k) - V(k-1)) \tag{3.11}$$

$$\Delta E = E(k) - E(k-1) \tag{3.12}$$

The output of the fuzzy logic converter is usually a change in the duty ratio of the power converter, ΔD, or a change in the reference voltage of the DC-link, ΔV. The fuzzy rule algorithm, associates the fuzzy output to the fuzzy inputs based on the power converter used and on the knowledge of the user. The advantages of these controllers, besides dealing with imprecise inputs, not needing an accurate mathematical model and handling non linearity, are fast convergence and minimal oscillations around the MPP. Whereas, the disadvantage of these controllers is that their effectiveness depends a lot on the skills of the designer for choosing the right error computation and coming up with an appropriate rule base.

3.1.6 Neural Network

Another MPPT method well adapted to microcontrollers is Neural Networks [18, 19]. They came along with Fuzzy Logic and both are part of the so called "Soft Computing". The simplest example of a Neural Network (NN) has three layers called the input layer, hidden layer and output layer, as shown in Fig. 3.3. The input variables can be parameters of the PV array such as $V_{oc}$and I_{sc}, atmospheric data as irradiation and temperature or a combination of these. The output is usually one or more reference signals like the duty cycle or the DC-link reference voltage. The main disadvantage of neural network technique is that the data needed for the training process has to be specifically acquired for every PV array and location. The characteristics of the PV array vary depending on the model and the atmospheric conditions depend on the location. These characteristics also change with time, so the neural network has to be periodically trained.

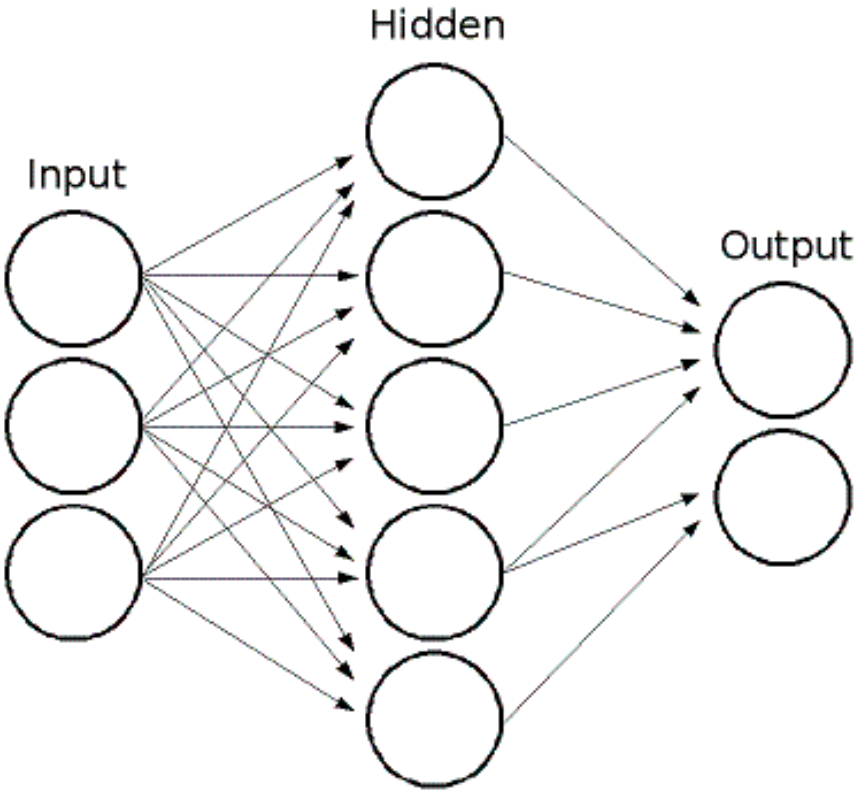

Fig. 3.3 Neural Network algorithm

3.2 MATLAB/SIMULINK Implementation of MPPT with Boost Converter

A DC-DC converter is used between the PV module and the DC bus to extract the maximum available power. It has been studied that the efficiency of the DC-DC converter is maximum for a buck converter, then for a buck-boost converter and minimum for a boost converter [20], but as the study intend to connect ship's ac load to the PV panel which required DC link voltage to be stabilized at 335V, therefore, a boost converter topology is utilized for implementation of MPPT algorithm in this study.

In line with the project requirement, Perturb and Observe algorithm for MPPT was implemented in MATLAB/SIMULINK environment using boost converter. The P & O technique was chosen over other algorithms owing to it being least complex and easily implementable scheme. As introduced in the previous chapters, 4 kW of power was determined to be the desired power output from the array for the simulation study for the proposed methodology. Fig. 3.4 presents the simulation result of the MPPT power output from the boost converter, and confirms the operation of the PV system at the

maximum power point, hence implementation of MPPT.

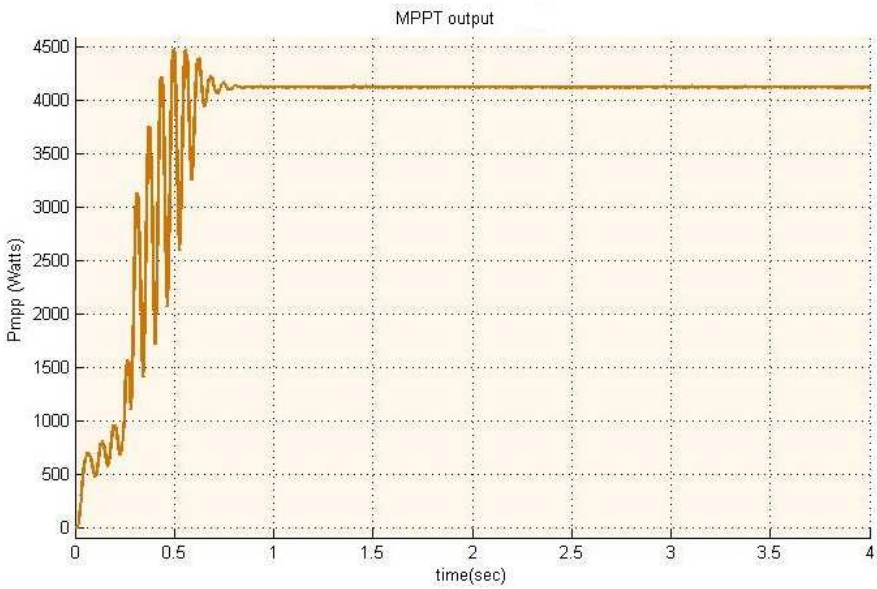

Fig. 3.4 Boost converter output depicting MPPT implementation

3.3 Conclusion

The chapter discusses the theory behind Maximum Power Point tracking and different ways of its implementation. Further, boost converter role in achieving MPP is discussed with elaboration of its mode of operation. Besides, the chapter also brings out Matlab/Simulink implementation of MPPT technique using boost converter and its importance in the present set up.

Chapter 4

MODELLING OF BATTERY CHARGING AND DISCHARGING CIRCUITS

4.1 Introduction

Rechargeable batteries are in wide use in standalone photovoltaic (PV) systems to store energy surplus and supply the load in case of low renewable energy production. Energy storage systems can assist in greater penetration of wind or PV as source of energy, reducing the diesel fuel consumption costs, as well as avoiding voltage and frequency variations. The scheme of operations as proposed in the present study requires an energy storage device to store the surplus energy, harnessed from installed photovoltaic system onboard solar ship. The PV system is perpetually operated at the maximum power point, employing the MPPT algorithm, thus allowing the system to provide the maximum surplus energy to store in the energy storage devices (ESD's) at all times. Battery among all energy storage devices is the most important energy storage device owing to its stable power supply capability.

Use of different type of batteries based on type and cost of application is prevalent. Lead acid battery (LAB), Lithium ion batteries and flow batteries are in common utilization among the others. The lead acid battery is the market leader owing to its large availability, flexibility in sizes and design, relatively higher efficiency and low specific costs. However, low life cycles, limited energy density, hydrogen evolution and high maintenance cost are some of its disadvantages. Lithium ion is another promising contender in the pack with high energy density, little or no maintenance requirement, low self discharge, high energy efficiency, longer life times and large number of cycles. However, need of protective circuit, high initial costs and thermal runaway when overcharged or crushed are some of its turn downs. Another promising battery and relatively in its formative stage on a commercial scale is the redox flow batteries [21, 22, 23]. These batteries have high cycle stability, low self discharge and are suitable for long term storage [24, 25]. However, being in its formative stage, the technology comes

with low energy density, complex control strategies and risk of leakages as it requires pumping of the electrolyte in a piping system.

The present study has considered lead acid battery as the part of energy storage system due to lower cost of implementation and its higher efficiency. The redox flow batteries, however, an attractive option for the study is left out due to its large space requirement. The literature also brings out the implementation of hybrid energy storage systems to cater for varied load profiles [26, 27, 28]. The use of fuel cells and super capacitors in conjunction with the batteries is extensively studied. Hybrid energy storage system inclusion to the proposed set up is foreseen as a future scope to the present study.

Battery charging and discharging is a major part of the present study and is therefore covered elaborately in this chapter. The introduction of basic concepts of buck and boost converter are considered imperative at this point owing to its extensive employment in battery charging and discharging procedures. DC/DC buck converter is utilised in battery charging circuit, while boost converters are critical component of battery discharging circuit. Since, batteries in a PV generation system is required to be from PV panel via DC link, it is required that DC link voltage is stepped down to a level comparative to battery terminal voltage for better control battery charging current. Similarly, while discharging, it is required that output voltage from the battery is comparable to DC link voltage for it to be able to support the DC link voltage for system operation. Thereby, a boost converter is employed in the discharging circuit. Different modes of operation of both buck and boost converters are covered subsequently as part of modelling of charging and discharging circuit respectively.

4.2 Modelling of Battery Charging Circuit

4.2.1 DC/DC Buck Converter

Circuit of the buck converter is shown in Fig.4.1. The fundamental circuit for a step down converter or buck converter consists of an inductor, diode, capacitor, switch with switch control circuitry. The circuit for the buck regulator operates by varying the amount of time in which inductor receives energy from the source. In the operation of the buck converter or buck regulator can be seen that the output voltage appearing

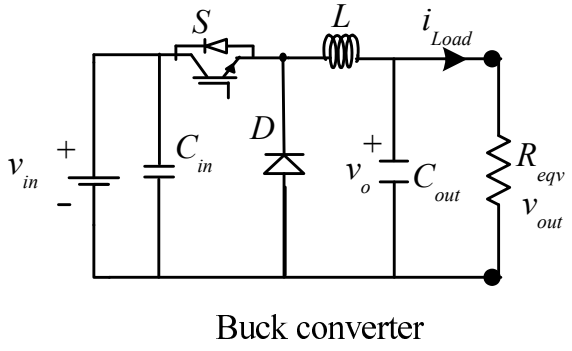

Fig. 4.1 DC-DC Buck converter

across the load is sensed by the sense / error amplifier and an error voltage is generated that controls the switch.

There are two modes of operation of a buck converter based on the closing and opening of the switch. The first mode is when the switch in the buck regulator is on, the voltage that appears across the inductor is $V_{in} - V_{out}$. Using the inductor equations, the current in the inductor will rise at a rate of $\frac{(V_{in} - V_{out})}{L}$. At this time the diode D is reverse biased and does not conduct.The second mode is when the switch is open; in this case also, the current must still flow as the inductor works to keep the same current flowing. As a result current flows through the inductor and into the load. The diode, D then forms the return path with a current I_{diode}equal to I_{out} flowing through it. In this mode, the polarity of the voltage across the inductor has reversed and therefore the current through the inductor decreases with a slope equal to $\frac{-Vout}{L}$. The two modes of operation of the buck converter are elaborated in Figs. 4.2 and 4.3 with the help of a circuit diagram. On applying inductor volt second balance for mode I and mode II, we

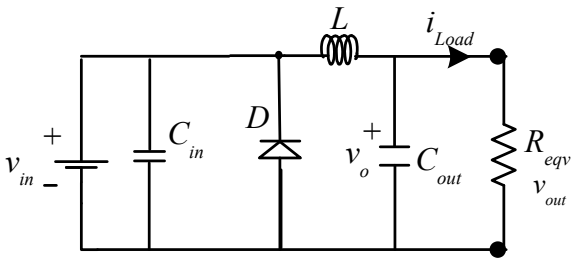

Fig. 4.2 Buck converter mode I

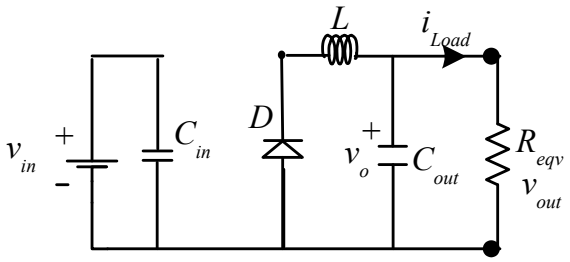

Fig. 4.3 Buck converter mode II

have,

$$(V_{in} - V_{out}) * t_{on} = -V_{out} * t_{off}. \tag{4.1}$$

And,

$$T = t_{on} + t_{off}. \tag{4.2}$$

Also, t_{on}/T is called the duty cycle α and therefore,

$$\alpha = t_{on}/T \tag{4.3}$$

From equation4.34

$$V_{out} = \alpha * V_{in} \tag{4.4}$$

where,

V_{out}- output voltage

V_{in}- voltage input

t_{on}- duration of time when the switch is closed.

4.3 Battery Charging Control

The expected battery lifetime is reduced if there is low PV energy availability for prolonged periods or improper charging control, both resulting in low battery state of charge (SoC) levels for long periods of time. The overall system cost can be reduced by the use of proper battery charging/ discharging control techniques, achieving higher SoC and consequently longer lifetime. Different battery charging approaches has been

studied in the literature [29] and are subsequently described.

4.3.1 Battery Charging with Direct Connection to PV System

In this case the battery is supplied with maximum available PV current, which depends on the battery state of charge [30]. On reaching a preset overcharge limit battery is disconnected from the power source. Other variants of this approach includes providing full PV array current to the battery until battery voltage reaches a set point, after which the voltage is either regulated at this value or reduced to a lower floating voltage for finishing the charging process. Disadvantage of this procedure is that the set point does not always coincide with the 100 percent state of charge condition. This is because, overcharging voltage depends on charge rate which depends on atmospheric conditions. Battery therefore, remains in floating charge state for a longer time to be fully charged.

4.3.2 On/Off Control for Battery Charging

The technique utilizes the control on battery charging current [31]. After battery voltage rises above the end point charge voltage, the aim is to regulate the battery voltage to a lower floating voltage level. The battery charger limits the battery current using on/off control to regulate the battery voltage to an upper set point after battery voltage reaches lower set point. Disadvantage of this method is that no energy is transferred to the battery during the off state, resulting in increasing the time for the battery to finish the charge process.

4.3.3 Ampere Hour Measuring Battery Charging Algorithm

This approach of battery charging depends on calculation of the state of charge (SoC) [32]. A management system monitors the SoC and gradually reduce the energy taken from the battery (i.e., reduce the load) to help prevent continuous operation at a low state of charge. The battery state of charge is estimated as following

$$SoC_{k+1} = SoC_k + \sum_t (I_{bat}(t) - I_{gas})\Delta t/C \tag{4.5}$$

where,

SoC_k and SoC_{k+1} are battery state of charge at k and k+1 respectively.

$I_{bat}(t)$ is the battery current.

I_{gas} accounts for the battery losses.

Δt is the time interval.

C is the nominal capacity of the battery in ampere hours.

The problem using this method is the effect of current measurement error on determination of SoC and battery lifetime.

4.3.4 Battery Charging with Reducing Charging Rates

It is observed that cell overcharges at about 2.4 V/cell, irrespective of charge rate. However, the 100% state of charge condition is achieved only when overcharging condition is reached with C/100 charge rate. In this case, battery current is monitored and limit is set on the maximum permissible charging current. The actual charging current can be equal to or less than this maximum current. However, battery charging current is a function of PV power produced and battery voltage depends on battery charging current and its state of charge. In order to ensure maximum permissible current for battery charging, MPPT algorithm is implemented in order to extract maximum power from the available solar panels. In this scheme of battery charging, the battery voltage is continuously monitored for overcharging condition. When the battery is charged to overcharging voltage, the maximum permissible battery current or the reference is reduced by a fixed step. The procedure is repeated until the battery current reference or the maximum permissible battery charging current is reduced to C/100. In this state, overcharging condition indicates 100% state of charge. The method offers many advantages as better exploitation of PV power as it allows the set up to operate at MPPT. Secondly, battery maximum SOC is achieved in least possible time. Also, it being battery current regulation method allows uniform charging of all cells hence can be effectively used for large battery strings.

A schematic diagram illustrating the battery charging procedure is presented at Fig. 4.4 and for further elaboration a control algorithm flowchart is given at Fig. 4.5. In this study, a buck converter is interfaced to the DC link which in turn is energized by the PV array, and a control unit is used to control the battery charging process. The

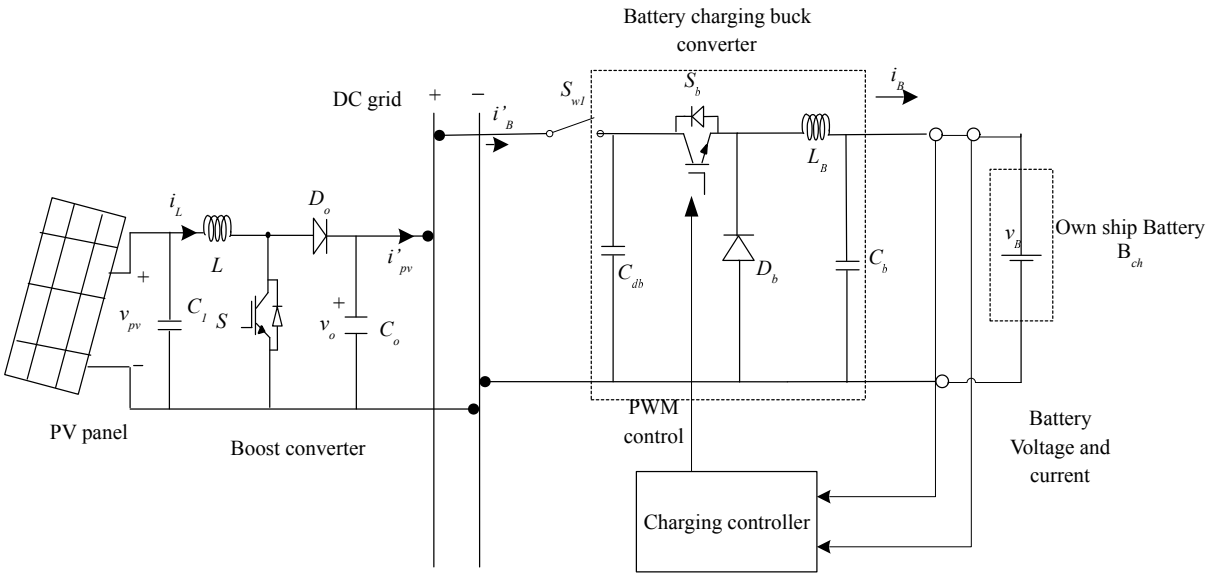

Fig. 4.4 Schematic of battery charging circuit

maximum battery current is set to $C/5$, where C is battery capacity in ampere hours, for protection of battery from overheating, and the minimum current is set to $C/100$ corresponding to a battery 100 % SoC. When the battery is fully charged the battery charging current is regulated to $I_{trickle}$, to compensate for the control system power consumption and the battery self discharge [29]. With reference to the flowchart at Fig. **??**, sequence of control actions performed to regulate the battery charging process are as follows,

- If battery current higher than maximum battery current, control action is to reduce battery charging current.
- If battery voltage rises above maximum voltage level, i.e., overcharge state, battery charging current is reduced. When the maximum battery current, i.e., the reference reaches $C/100$ level, indicating 100 % SoC, maximum battery current is set to $I_{trickle}$.
- If battery voltage is below minimum voltage level, the maximum battery charging current is restored.

Further, when the battery charging current must be reduced, the duty cycle must be reduced, i.e.,

$$D_{k+1} = D_k - |\Delta D| \tag{4.6}$$

To prove that duty cycle reduction causes regulation of battery current to desired level following analysis is undertaken. When converter operates in CCM, the input and out-

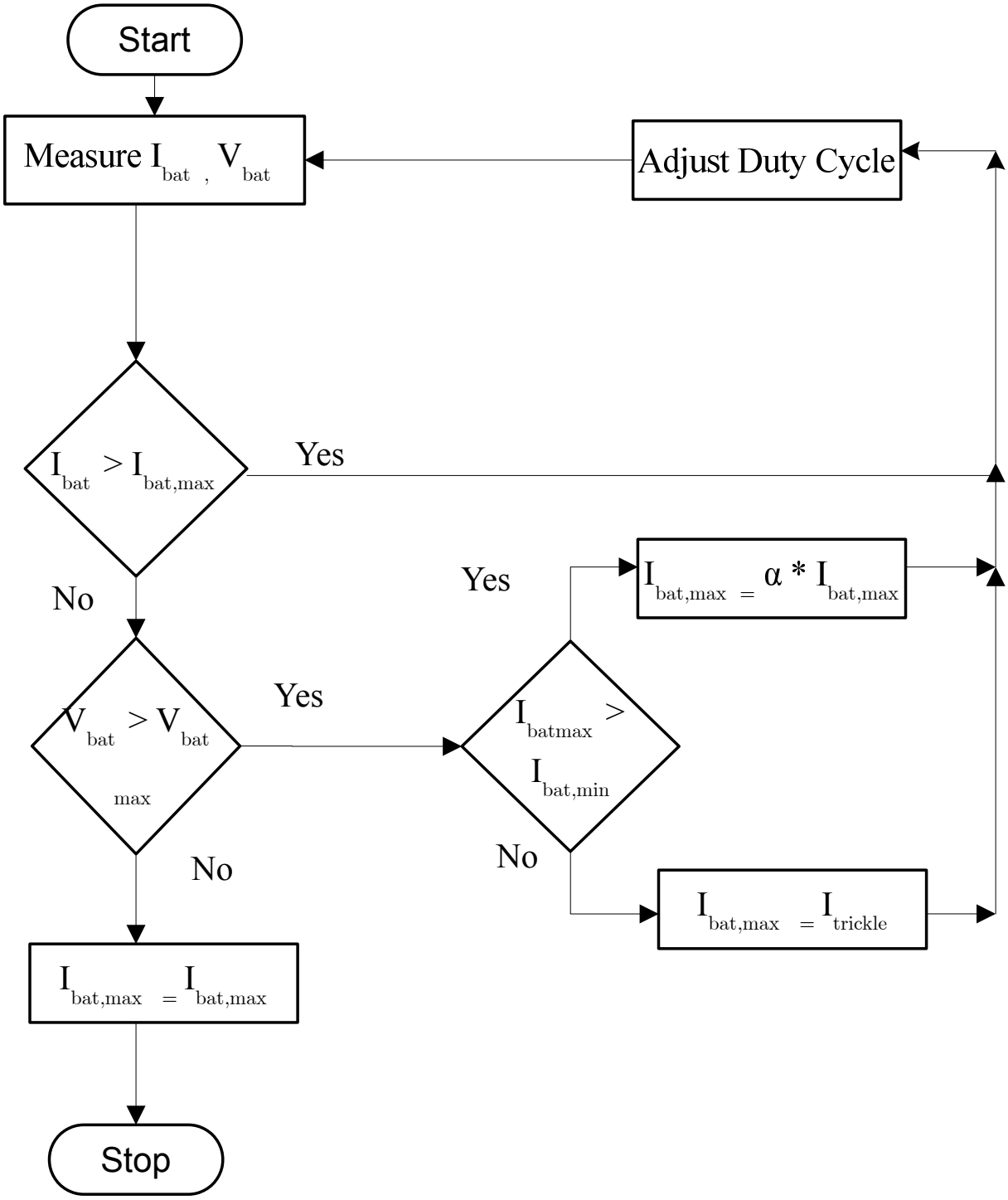

Fig. 4.5 Control algorithm flowchart

put voltage levels are related as follows,

$$D = \frac{V_o}{V_{in}} \tag{4.7}$$

and

$$\frac{dD}{dV_{in}} = -\frac{V_o}{V_{in}^2}. \tag{4.8}$$

Where, V_o and V_{in} are the DC/DC converter input and output voltage levels, respectively and D is the PWM control signal duty cycle value. Thus, a duty cycle reduction causes a o PV array output voltage increment, which moves down the hill shaped curve, thereby regulating the battery charging current below the maximum battery current value.

4.4 Modelling of Battery Discharging Circuit

4.4.1 DC/DC Boost Converter

Circuit of the boost converter is shown in Fig.4.6. The converter is controlled

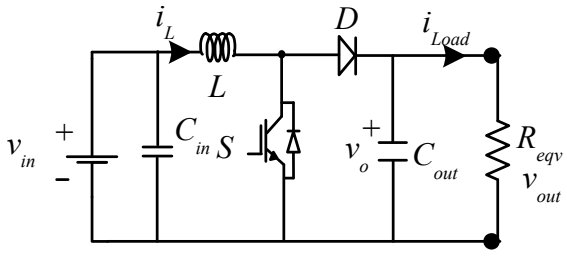

Fig. 4.6 DC-DC Boost converter

through a closed loop voltage controller [33, 20].The power switch is responsible for modulating the energy transfer from the input source to the load by varying the duty cycle D. In this light, it is understood that there are two modes of operation of a boost converter based on the closing and opening of the switch. The first mode is when the switch is closed; this is known as the charging mode of operation. The second mode is when the switch is open; this is known as the discharging mode of operation. The two modes of operation of the boost converter are elaborated in Figs. 4.7 and 4.8 with the help of a circuit diagram. On applying inductor volt second balance for mode I and mode II, we have

$$V_{in} * t_{on} = (V_{out} - V_{in}) * t_{off} \tag{4.9}$$

And,

$$V_{out} = ((t_{on} + t_{off}))/t_{off} * V_{in} \tag{4.10}$$

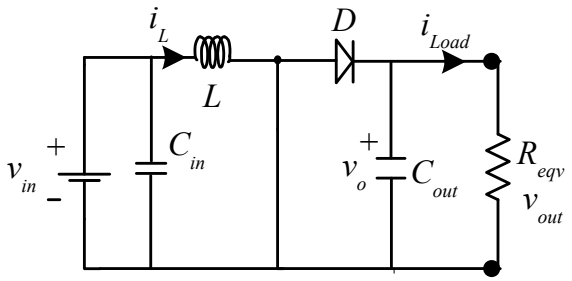

Boost converter Mode I

Fig. 4.7 Boost converter mode I

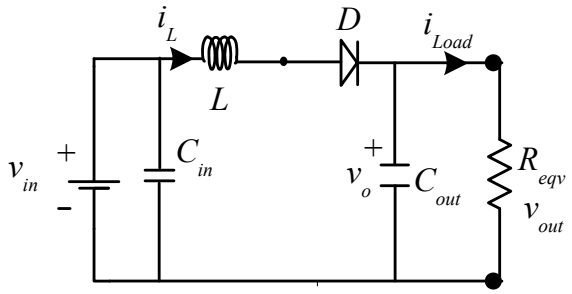

Boost converter Mode II

Fig. 4.8 Boost converter mode II

where,

$$T = t_{on} + t_{off} \tag{4.11}$$

Also, t_{on}/T is called the duty cycle α and therefore,

$$\alpha = t_{on}/T \tag{4.12}$$

From equation4.19

$$V_{out} = 1/((1-\alpha)) * V_{in} \tag{4.13}$$

where,

V_{out}- output voltage

V_{in}- voltage input

t_{on}- duration of time when the switch is closed

4.4.2 Requirement of Modified Boost Converter

Conventional boost converter when operated in continuous conduction mode (CCM), the reverse recovery current of output diode D_o has a detrimental effect on performance of converter. During turn on of the power switch in mode I of boost converter, the output diode reverse recovery current I_{rr} induces additional turn on loss due to overlapping of high current and voltage. Further, switch current stress is increased by reverse recovery current and diode voltage stress increases due to parasitic inductance in output diode loop.

Many possible solutions for the said problem has been discussed in literature [34]. One of the solution is operation in DCM mode. However, due to high peak current in power devices, conduction losses and current stress on power devices increases in DCM mode. Another possible remedy is reducing switching frequency for CCM operation. Due to low power density in this case, it is not preferred. Use of high performance devices like Sic diodes is another way of dealing with problems of conventional boost converter, but is an expensive method. Further, soft switching of the diode i.e., controlling diode turn off current falling rate is another popular method which tags along increased complexity and circuit cost. Finally, use of leakage inductance of coupled inductor in series to control output diode current falling rate when switch is turned on is the most economical method to solve the reverse recovery problem and is used in the modified converter utilised for this study. The said converter is subsequently described in this chapter.

4.5 Modified Boost Converter with Coupled Inductor and Superlift Techniques

A PV battery hybrid power system generally consists of a PV generator (solar panels), battery bank, a bi-directional converter for battery charging and discharging, inverter and ac load. In view of the present study, the PV generation system sub sections include PV array, MPPT boost converter, buck converter with charging current control for battery charging, coupled inductor battery discharging circuit, DC load in the form of external ship/ target ship battery and own ship ac load. Now the required

rms voltage at single phase at ac load bus is 230, 50 Hz. In order to avoid over modulation and considering loses at LC filter, 300 V dc is required to maintain 230 V rms at load bus [35]. As is brought out in earlier chapters, the set up utilizes complimentary batteries wherein one set of batteries is at all times supporting the dc link voltage. The designated battery, therefore, discharges through a coupled inductor boost converter to assist in maintaining the dc link voltage in presence and absence of PV panel that is both during day and night time scenarios. However, as is brought out in the results of the study, the control objective varies for the night time cases i.e., connection of target ship battery to own ship battery and catering of ship's ac load from the charged battery. While, the former case the set up strives to maintain target ship charging current, in the later aim is to maintain the inverter output voltage.

The present study proposes the use of a separate battery discharging circuit instead of a bi-directional DC/DC converter for battery charging, as the proposed set up allows easy implementation of charging current control algorithm and to cater for utilization of lesser number of batteries (unitary 48 V battery) during the discharge mode. It is now a common knowledge that electricity produced by renewable energy sources change randomly due to random change in environmental conditions. For example, A PV generation system is susceptible to weather condition and location [36]. A high step up coupled inductor boost circuit can generate a DC bus with a battery bank which allows the set up to cater for simultaneous charging of own ship battery and cater for ship's AC load.

In general, step up DC/DC converters are classified in two main categories, i.e., isolated and non-isolated converters. Forward, flyback, push pull, half bridge and full bridge are the isolated converters and offer a high gain on adjustment of the turns ratio. The shortfall of these converters is the high voltage spike and considerable power loss in the main switch owing to the leakage inductance. Utilization of active clamp circuits to counter the shortcomings in turn increases the cost and complexity of the circuit. Amongst the non isolated topologies boost converter is a step up topology, however, it is not suitable for high step up DC/DC conversion because of considerable switching loss and reverse recovery problem in scenarios with high converter gain [37, 38, 39, 40].

The inherent issues with the boost converter topology are addressed in the coupled inductor topology with adjustment of turns ratio of coupled inductor and recycling of the energy of the leakage inductor. As a result, high voltage gain, high efficiency and

low off state voltage for the main switch can be achieved. In this study, a topology involving coupled inductor and super lift techniques is utilized. The super lift stage absorbs the leakage inductance energy, clamps the off state voltage of the main switch and provides a moderate voltage gain. On the other hand, coupled inductor technique provides a high voltage gain and alleviates the reverse recovery problem of the output diode. The topology of the converter as utilized in the set up is shown in Fig. 4.9 [2].

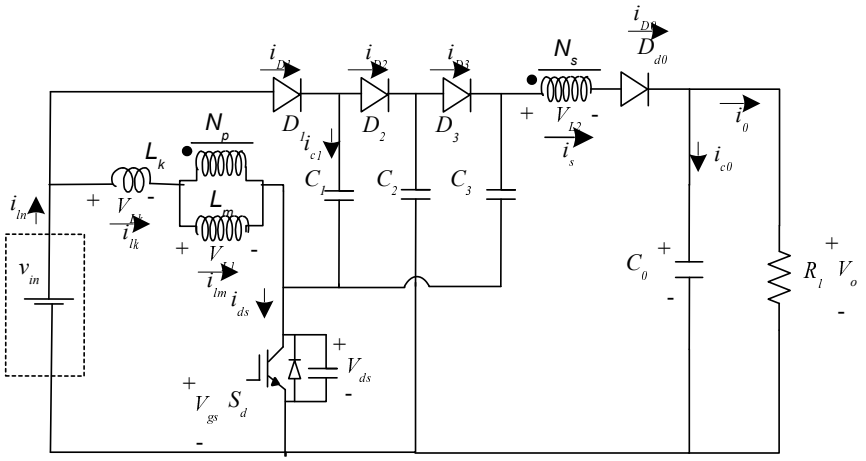

Fig. 4.9 Battery discharging circuit [2]

4.6 Operating Principle of Discharging Converter

Some assumptions are considered for bringing out the operation of the converter [2]. The capacitors are assumed to be large enough, so the voltages $V_{C1},\ V_{C2},\ V_{C3}$ and V_0 remain constant during a switching period. All diodes are considered to be ideal. Thirdly, the parasitic capacitor of the main switch is assumed to be non-zero. Also, the coupling coefficient of the coupled inductor and the turns ratio of the coupled inductor are defined as $k = \dfrac{L_m}{(L_m + L_k)}$ and $n = \dfrac{N_s}{N_p}$, respectively. Also, $n = \sqrt{\dfrac{L_1}{L_2}}$. Capacitors $C_1,\ C_2,\ C_3$ and diodes $D_1,\ D_2,\ D_3$ constitute the super lift stage and leakage inductance L_k, magnetising inductance L_m and ideal transformer are used to model the coupled inductor. During the coarse of operation, when the switch is off $D_2,\ C_1$ and C_2 absorbs the leakage inductance and clamp the voltage across the main switch to

$$V_{ds} = V_{c_2} + V_{c_1} \tag{4.14}$$

. C_1 and C_2 are connected in series in reverse polarity hence, their voltages are subtracted thereby, reducing the voltage across the main switch.

The operation of the converter in CCM mode is divided into five modes i.e mode I - V. Each of these modes with relevant circuit is provided subsequently for better understanding of the working.

4.6.1 Mode I

This mode starts with switching on of switch S. As shown in Fig. 4.10, diode D_0 stays forward biased, D_2, D_1 and D_3 is reverse biased. Due to leakage inductance of the inductor, secondary side current decreases with increase in i_{lk} thereby, controlling the diode current falling rate, hence, alleviating the reverse recovery problem. Further, C_0 is charged via L_1, C_3 and L_2. Also, capacitor C_1 gets charged by input DC voltage V_{in}. Therefore, sum of i_{lk} and i_{c1} flows through switch S. Capacitors C_2 and C_3 are connected in parallel and the former charges the later. Mode ends with i_{Do} achieving zero value.

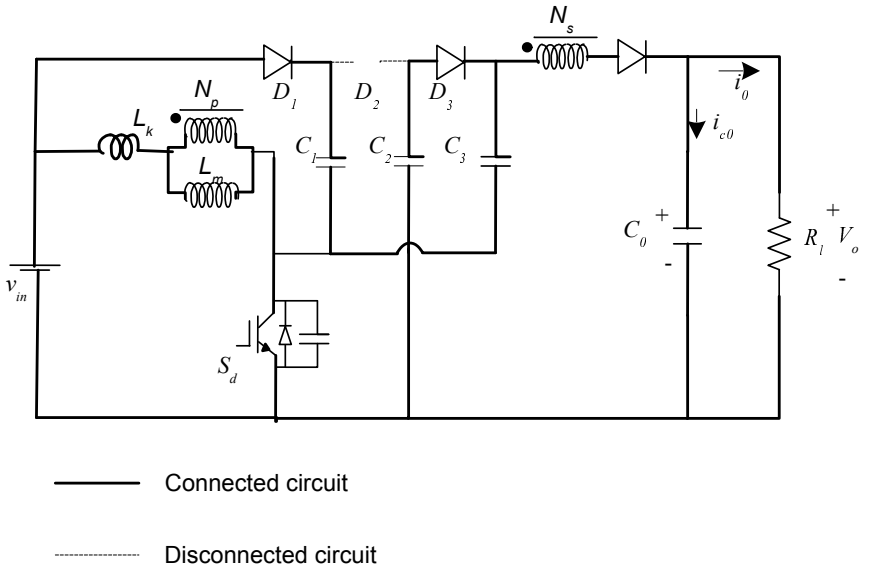

Fig. 4.10 Battery discharging circuit in Mode I

4.6.2 Mode II

With main switch S on, diodes D_1 and D_3 gets forward biased while diodes D_o and D_2 are reverse biased. The scheme of operations is brought out in Fig. 4.11. In this case, magnetizing inductance gets energized by input voltage source while the output capacitor C_o delivers its energy to the load. This mode ends with switching off of the main switch S.

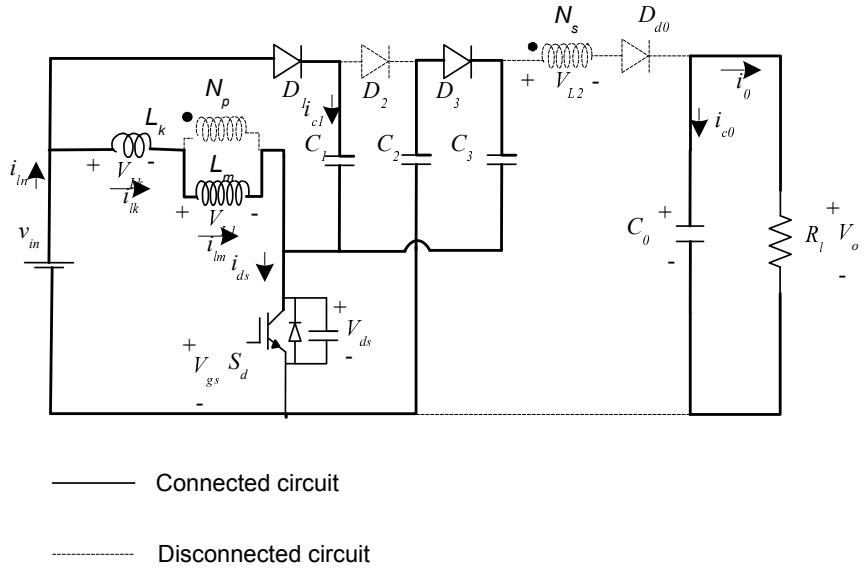

Fig. 4.11 Battery discharging circuit in Mode II

4.6.3 Mode III

With switch S turned off diodes D_1, D_2, D_3 and D_o gets reverse biased. Energy of both leakage inductance and magnetizing inductance is released to parasitic capacitor of the main switch. Therefore, voltage across S increases linearly. Also, C_o delivers its energy to the load as is shown in Fig. 4.12. Once, voltage across the main switch S, V_{ds} becomes more than $V_{c2} - V_{in}$ diode D_2 conducts, marking end of this mode.

4.6.4 Mode IV

In this mode, diode D_0 is also forward biased. The circuit as elaborated in the Fig. 4.13, shows capacitors C_1 and C_2 to be connected in series, while part of energy

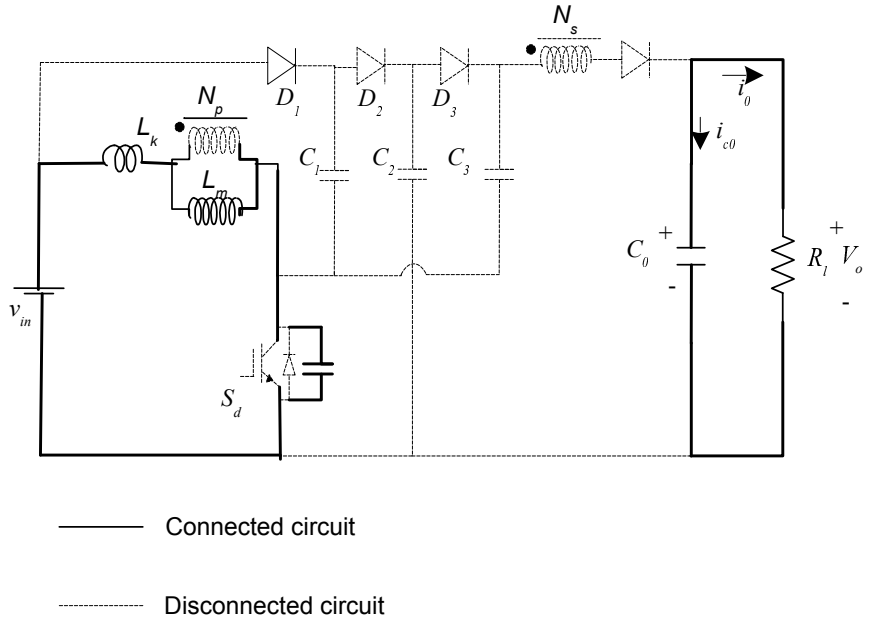

Fig. 4.12 Battery discharging circuit in Mode III

from leakage and magnetizing inductance is transferred to these capacitors. Besides, secondary side current i_s increases linearly, thereby, recycling the leakage inductance energy. The voltage stress at the switch is limited to $V_{c2} - V_{c1}$.

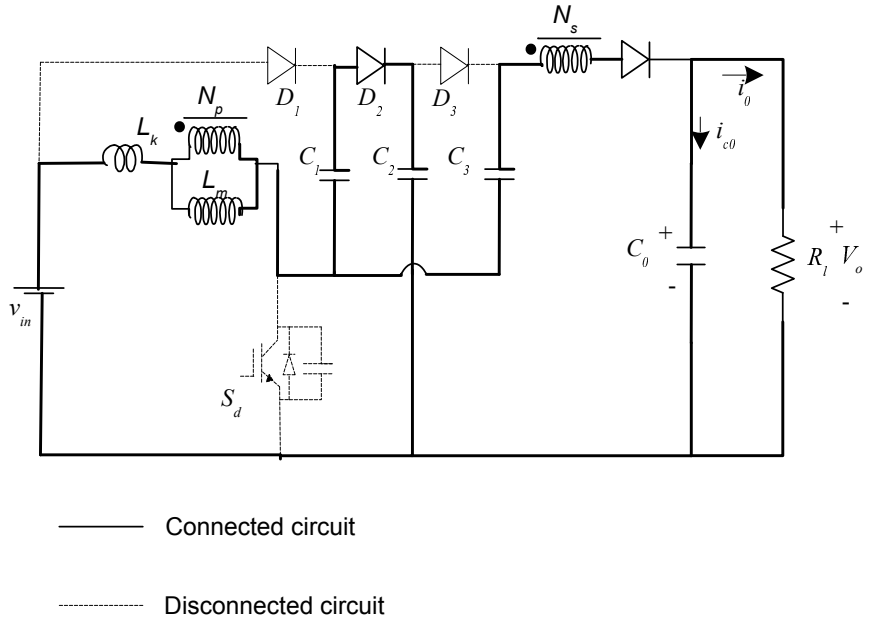

Fig. 4.13 Battery discharging circuit in Mode IV

4.6.5 Mode V

In the beginning of this mode i_{Do} equals i_{Lk}, therefore diode D_2 is reverse biased and only D_o is conducting. As shown in the Fig. 4.14, DC input voltage source, secondary side voltage V_{L2}, primary side voltage V_{L1} and V_{C3} are connected in series to charge the output capacitor and to provide energy to the load. This mode is ended with turning on of the main switch S.

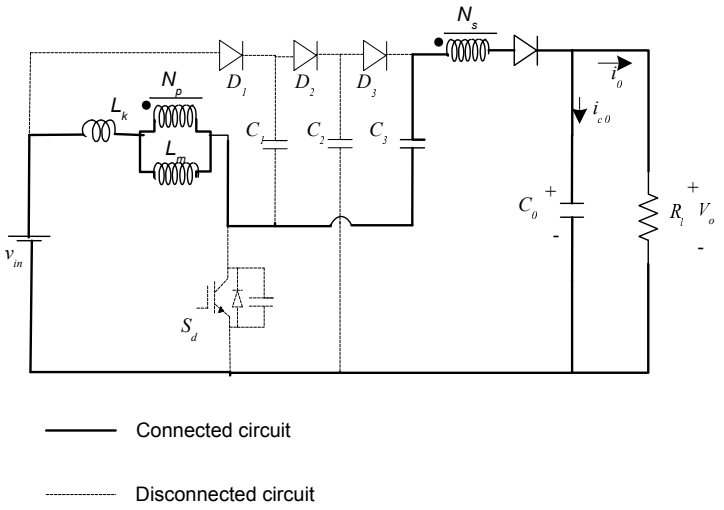

Fig. 4.14 Battery discharging circuit in Mode V

4.7 Steady State Analysis of Discharging Converter

To analyze the steady state behaviour of the proposed converter in CCM, the following procedure is performed. During mode II, the following equations for the voltages $v_{L_1},\ v_{L_2},\ v_{C_1}$ and v_{C_3} can be obtained from Fig. 4.11

$$v_{L_1}^{II} = \frac{L_m}{L_m + L_k} * V_{in} = kV_{in} \tag{4.15}$$

$$v_{L_2}^{II} = nv_{L_1}^{II} = nkV_{in} \tag{4.16}$$

$$v_{C_2}^{II} = v_{C_3}^{II} \tag{4.17}$$

$$v_{C_3}^{II} = V_{in} \tag{4.18}$$

During mode V, the following equations for the voltages v_{L_1} and v_{L_2} can be formulated from Fig. 4.14

$$v_{L_2}^{V} = V_{in} + v_{C_3} - V_0 - v_{L_k} - v_{L_1} \tag{4.19}$$

$$v_{L_2}^{V} = n v_{L_1}^{V} \tag{4.20}$$

In mode IV, according to Fig. 4.13 the following two equations can be derived

$$V_{in} = v_{L_k}^{IV} + v_{L_1}^{IV} - v_{C_1}^{IV} + v_{C_2}^{IV} \tag{4.21}$$

$$v_{C_2}^{IV} = v_{C_1}^{IV} - v_{C_3}^{IV} + v_{L_2}^{IV} + v_0^{IV} \tag{4.22}$$

Assuming that the capacitors C_2 and C_3 are large, the voltage across C_2 and C_3 can be obtained as follows

Now,

$$v_{L_1}^{IV} = k * (V_{in} + v_{C_1}^{IV} - v_{C_2}^{IV}) \tag{4.23}$$

$$v_{L_2}^{IV} = n * k * (V_{in} + v_{C_1}^{IV} - v_{C_2}^{IV}). \tag{4.24}$$

Also, v_{C_1} is charged to V_{in} prior to beginning of mode IV. Therefore,

$$v_{L_2}^{IV} = n * k * (2 * V_{in} - v_{C_2}^{IV}) \tag{4.25}$$

$$v_{C_2}^{IV} = V_{in} - v_{C_3}^{IV} + n * k * (2 * V_{in} - v_{C_2}^{IV}) + v_0^{IV}. \tag{4.26}$$

Dropping the superscripts and considering $V_{C_2} = V_{C_3}$, from mode II, we have,

$$2V_{C_2} + nkV_{C_2} = V_{in} + V_0 + 2nkV_{in}. \tag{4.27}$$

Therefore,

$$V_{C_2} = V_{C_3} = \frac{V_0 + V_{in} * (2kn + 1)}{nk + 2} \tag{4.28}$$

Further, for determining gain of the converter, considering only modes II and V and applying volt second balance on primary side winding of coupled inductor N_P, as follows

$$\int_0^{DT_s} v_{L_1}^{II} + \int_{DT_s}^{T_s} v_{L_1}^{V} = 0 \tag{4.29}$$

Now, Using (4.15), (4.19), (4.28) and (4.29)

Also, V_{Lk} can be derived as follows

$$V_{Lk} = \frac{1-k}{k} * V_{L_1}. \tag{4.30}$$

Substituting eqn. 4.30 and 4.28 in eqn. 4.19, we have

$$v_{L_1}^{V} = \frac{k}{nk+2} * [3V_{in} - V_0]. \tag{4.31}$$

Further, using eqn. 4.29, the voltage gain for the converter can be derived as follows

$$\frac{V_0}{V_{in}} = \frac{[3 + D(nk-1)]}{(1-D)}. \tag{4.32}$$

For an ideal case value of k is unity, i.e., maximum coupling and equation for gain becomes,

$$\frac{V_0}{V_{in}} = \frac{[3 + D(n-1)]}{(1-D)}. \tag{4.33}$$

Now, considering, n = 1,

$$\frac{V_0}{V_{in}} = \frac{3}{(1-D)}. \tag{4.34}$$

The value obtained at (4.34), is thrice the gain obtained by conventional boost converter. Besides, for n = 0.24 and k = 1 and a duty cycle of 0.63, gain obtained in this study is 6.875, i.e., for an input voltage of 48 V, output of 330 V was achieved.

4.8 Simulink Implementation of Battery Charging Circuit

Battery charging with reducing charging rates is utilized as part of battery charging circuit of the set up, due to its listed advantages. The charging circuit of the own ship battery is connected to the PV panel in both the day time scenarios when PV panel

supports the ship AC load or charges the target ship battery. The simulation set up provides for a complimentary battery set up, wherein, while one battery set charges from the PV panel, the other set of batteries support the DC link voltage by disconnecting the charging circuit and connecting the coupled inductor discharging circuit (discussed in the next section). Implementation of this scheme of events allows for a stable DC link voltage and thereby allowing non fluctuating voltage across charging battery and single phase inverter catering the AC load. The battery charging circuit is implemented using a buck converter controlled by charge current controller algorithm which monitors the battery voltage and manipulates the reference current values for battery charging current. This reference current is then passed to a PI controller, output of which is further pulse width modulated to generate gating signals for the Insulated Gate Bipolar Transistor (IGBT), controlling the buck converter operation. For simulation 50V is set as overcharging voltage for the connected 48V battery and the charging current is reduced in steps every time battery voltage reaches 50 V. Step reduction in charging current , voltage and corresponding SOC curve as obtained from simulation is shown in Fig. 4.15 - 4.17. From the curves, it is evident that charging current reduces every time battery voltage reaches the overvoltage mark hence, allowing the battery to be charged at a lower rate to achieve 100% charged state.

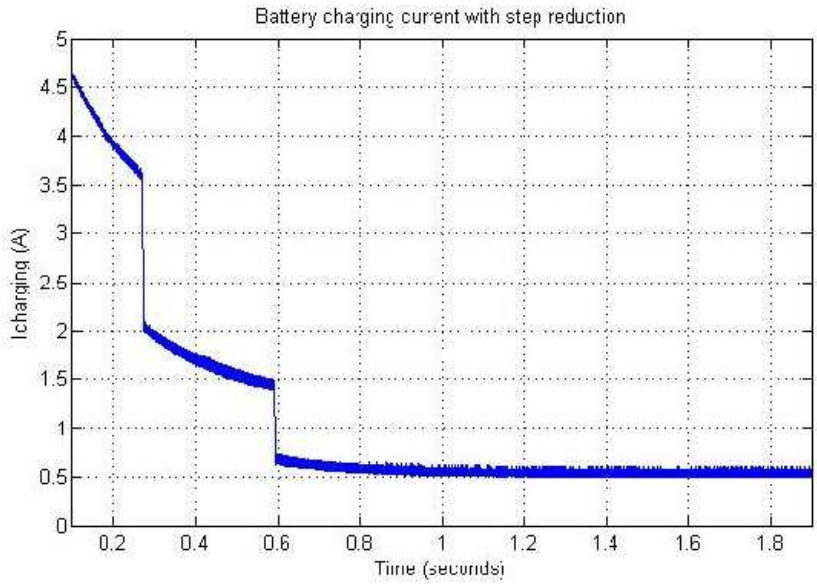

Fig. 4.15 Step reducing Battery charging current

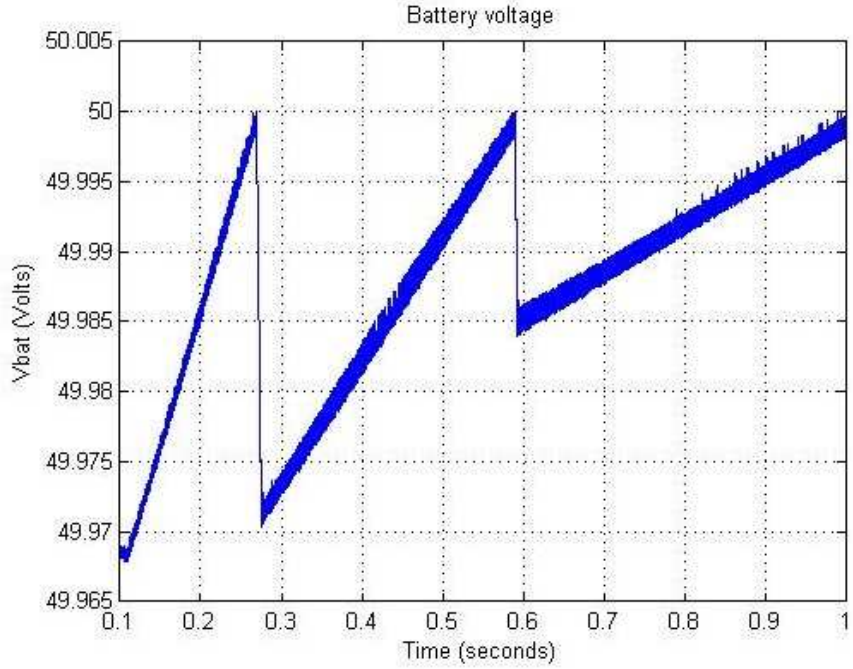

Fig. 4.16 Battery charging voltage

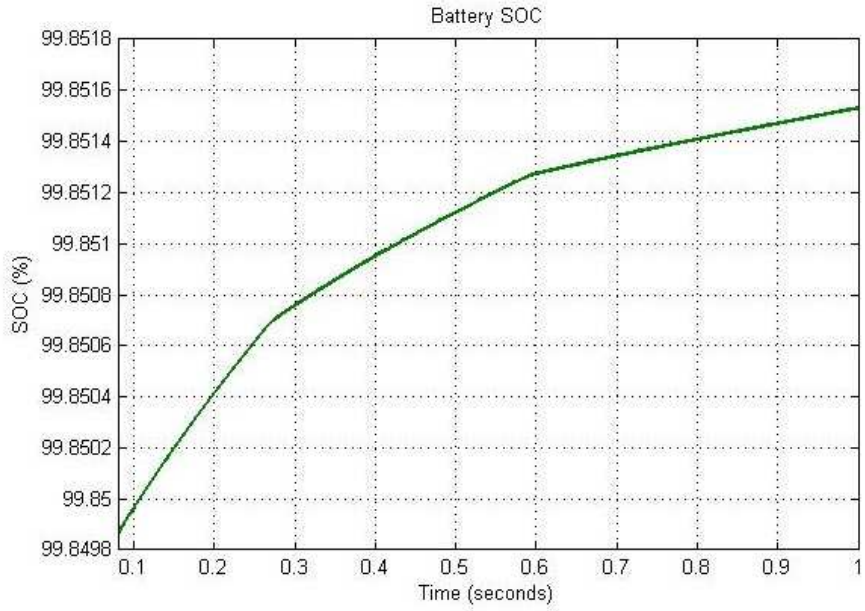

Fig. 4.17 Battery SOC

4.9 SIMULINK Implementation of Battery Discharging Circuit

In order to implement the discussed converter in MATLAB/Simulink, a pre-requisite of maintenance of DC link voltage to an acceptable range of values was set in order to

be able to connect AC load to the PV generation system. Similarly, when operating to cater for DC loads like target ship battery, aim was to maintain an acceptable range of charging current for the target ship battery. To achieve the set objectives, it was observed that changing of load resistance values for the converter was required based on the different modes of operation (discussed in the next chapter) and available insolation values. However, to limit the scope of study, insolation value was kept fixed during the course of study. The gate signal for the main switch S is controlled using PI controller, generating proportional values based on error values of discharging current when compared to the reference signal. The output of the PI controller is further processed with Pulse Width Modulation (PWM) technique to generate the requisite gate signal to achieve boost action of the converter. Voltage input and output curves illustrating the boost action of the described converter for a case when PV is charging both own ship battery and target ship battery is shown in Fig. 4.18 and for a case when PV is charging own ship battery and ship's AC load is shown in Fig. 4.19. Fig. 4.20 brings out the performance of the boost converter for a case when battery caters for ship's AC load in the absence of PV.

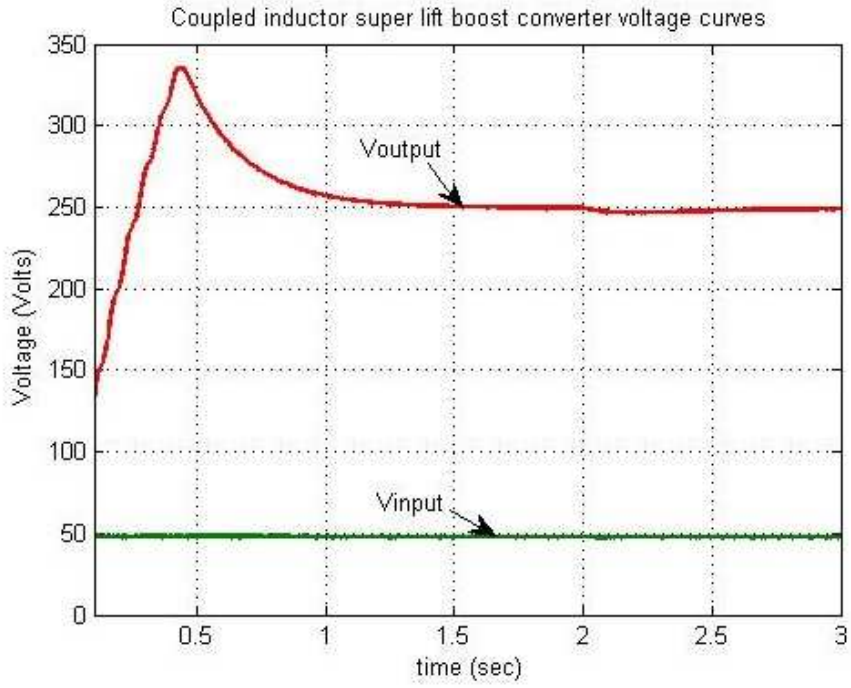

Fig. 4.18 Voltage curve PV charging own and target battery

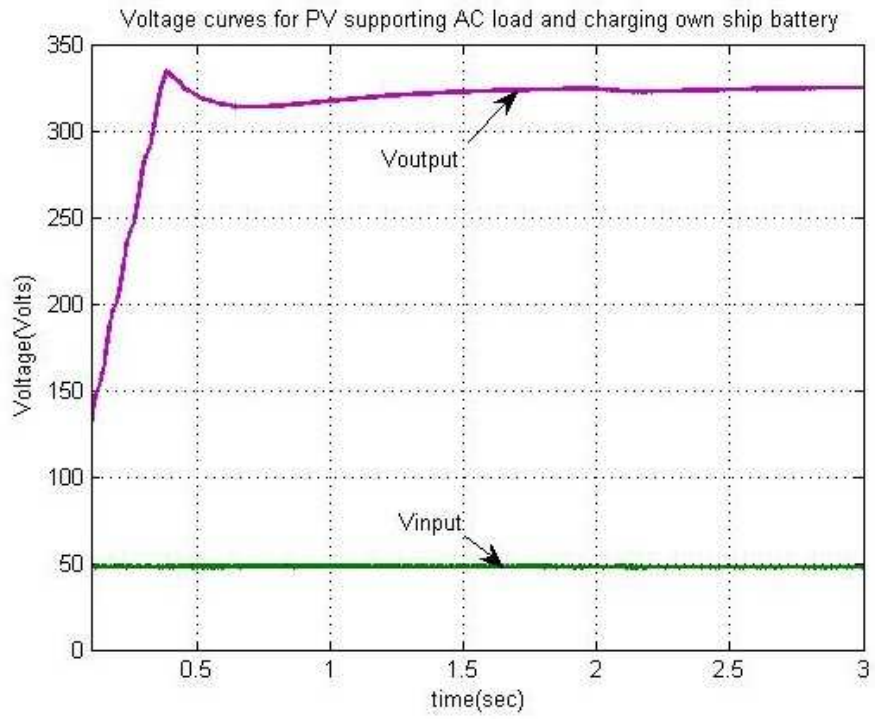

Fig. 4.19 Voltage curve PV charging own battery and catering AC load

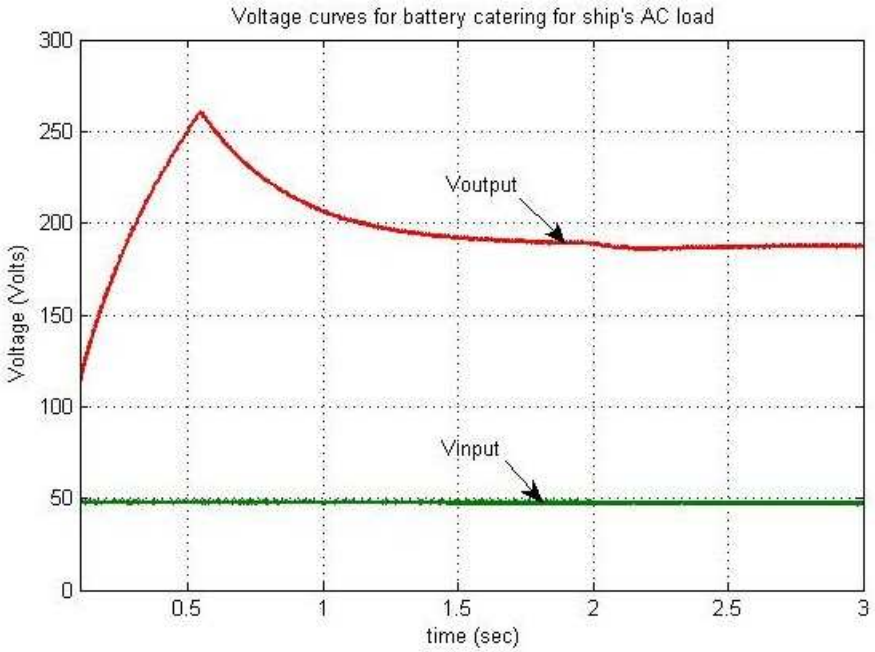

Fig. 4.20 Voltage curve own battery catering AC load

4.10 Conclusion

The chapter discusses different battery charging techniques and the implementation of battery charging using stepped reduction in current. Further, the battery dis-

charging circuit utilizing coupled inductor boost converter with super lift techniques is discussed in detail to bring out its working and Matlab/Simulink implementation.

Chapter 5

MODES OF OPERATION AND SIMULATION RESULTS

Basic components of generalized structure of standalone power system based on renewable energy sources are energy generator like PV generator connected to a DC/DC converter controlled by MPPT algorithm to optimize the operation of the power source. In addition, there is an energy storage device connected to charging/discharging system to manage the DC bus. The DC bus is formed by the parallel connection of the DC/DC converter output and is further connected to unidirectional or reversible loads. Therefore, it is required that such a bus provides a regulated voltage depending on the load requirements. The main objective of control system associated to the bus voltage regulator is to control the output voltage of the charging/discharging circuit to guarantee stability [41]. Previous studies available in the study suggest the use of non linear controller like sliding mode control to guarantee global stability of the DC bus in any operation condition [42]. However, the present study utilizes classical linear control techniques like PI controllers to limit the complexity of the study.

In relation to the study undertaken, cue is taken from many configurations available in literature for connection of PV source, battery storage, DC load and AC load. Many studies primarily discuss about the use of bi directional DC- DC converters for charge and discharge of the battery storage [43, 44]. In contrast, a separate charge and discharge circuit was utilized for the present study to achieve better control on battery charging and ability to vary load of the discharging circuit at the DC link based on the different operating conditions to achieve a required value of DC link voltage. The prior decision on mode specific load values is possible in this study because ship power system under study is a controllable power system with more or less fixed loading profile. Unlike a residential microgrid system, a ship power system exhibits conscious decision making of switching on equipments based on loading capacity.

It is understood that DC link voltage varies if there is a power mismatch between source and load. The cause of such a mismatch could be variation in solar irradiation

or changes in load values. It is therefore, required to maintain DC link voltage to a constant level in concordance with the load requirements irrespective of the changes. Discharging battery with its discharging circuit (boost converter) constitutes the DC-bus voltage regulator as it assists in maintaining the DC link voltage and enables the system to supply energy when main power source is not available or is unable to cater the load demand. The basic circuit configuration for the study undertaken is shown in Fig. 5.1. A schematic representation of the circuit is shown in Fig. 5.2. A flowchart bringing out the scheme of operations and conditions for applying different modes of operation as described further is given in Fig. 5.3.

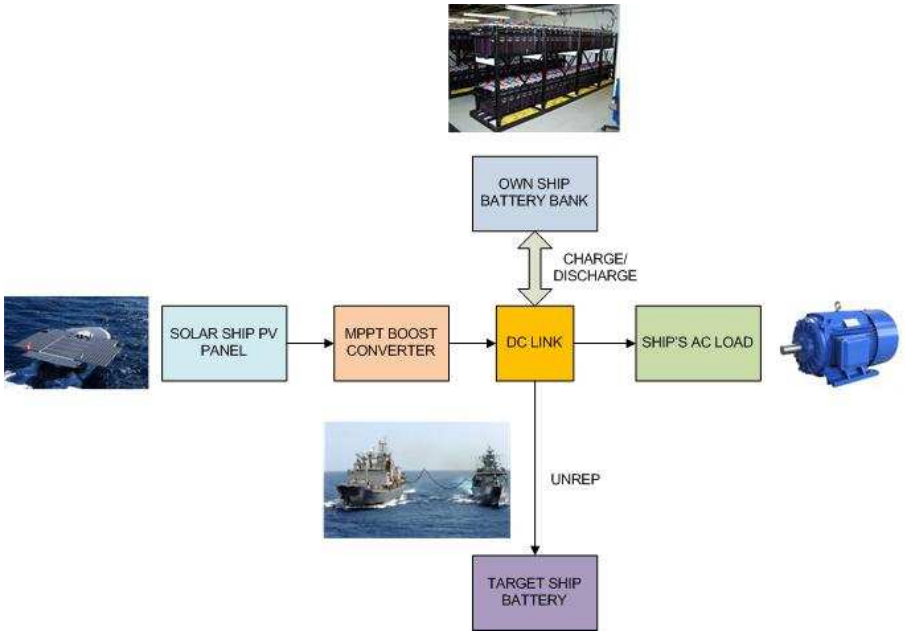

Fig. 5.1 Block diagram of circuit configuration for study

5.1 Modes of Operation

The study is undertaken under four cases, simulating the possible situations in day and night scenario. While modes I and II simulate the day time scenarios, modes III and IV simulate the night time scenarios. The operation of the model in day or night scenarios is undertaken with the help of manual control switch which connects or disconnects the PV panel to the circuit. Similarly, another manual control switch controls the connection of ship's AC load or DC load in the form of target battery depending on the occurrence or non occurrence of UNREP. Such a control is envisaged

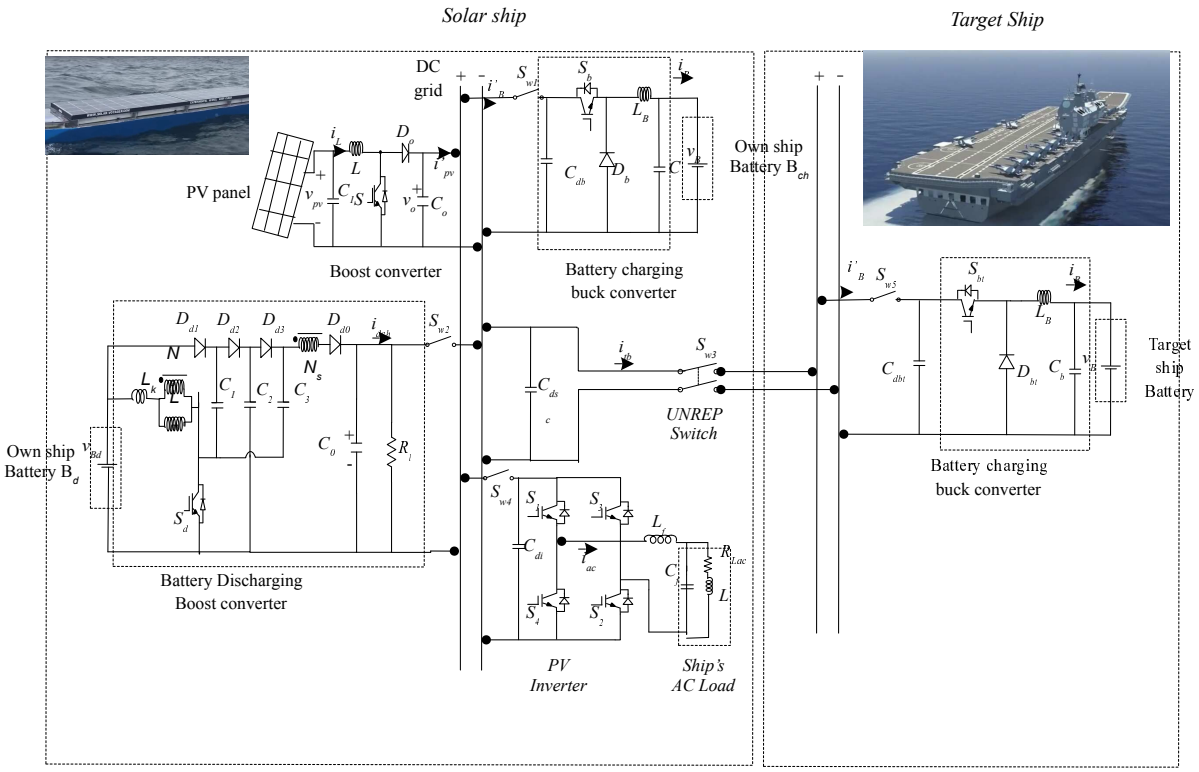

Fig. 5.2 Schematic representation of circuit

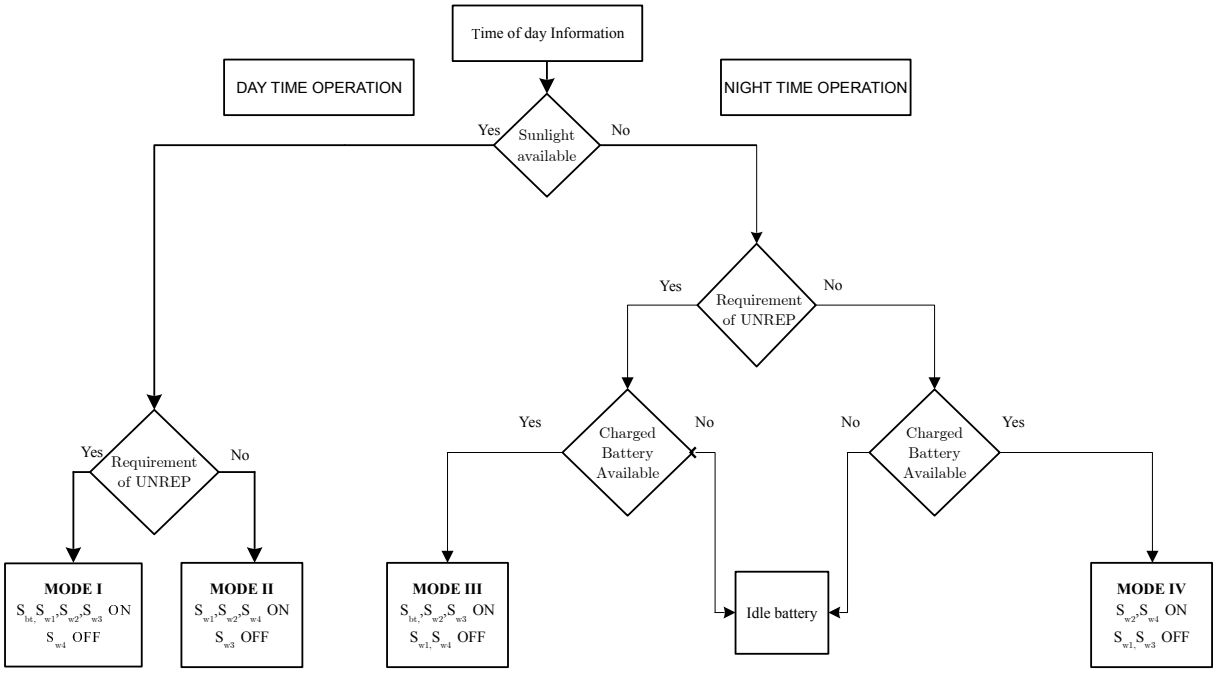

Fig. 5.3 Criteria for modes of operation.

to be present onboard ship, wherein target battery is connected to the system only under UNREP evolution. Each of the four cases is further elaborated subsequently in the discussion with relevant block diagrams to illustrate the operation modes.

5.1.1 Case I: PV Charging Target Ship Battery and Own Ship Battery

This case elaborates a day time scenario wherein PV power is available and UNREP operation is undertaken at sea between the solar ship and the target ship. In this study, own ship battery bank is such connected that during all day scenarios there exists a complimentary set of batteries, wherein, one set charges from the available PV energy the other battery supports the DC link voltage and provides for the deficient energy in case of a shortfall. The aim of such a set up is to maintain the DC link voltage to a constant level. The set up also allows the PV generation system to operate at MPP at all times thus maximum available energy is harnessed from the solar panels. As brought out in the previous chapters during UNREP procedure a cable is passed between the two ships for transfer of fuel. In this scenario, transfer of electrical energy from the solar ship to the target ship is simulated. Illustration of the connected circuit in this case is shown in Fig. 5.4. It is also to be observed that PV does not cater for ship's AC load during UNREP evolution and is only connected to the DC load.

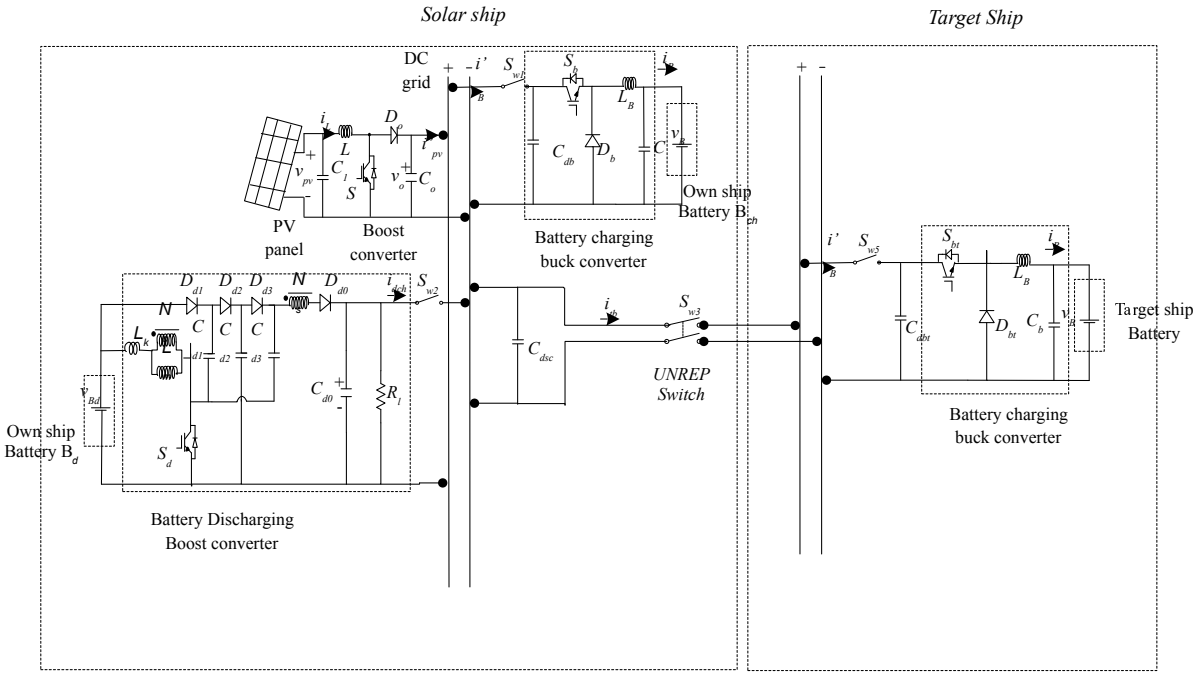

- Mode I : PV charging own ship battery and target ship battery.
- Ship's AC load not connected in this mode.
- Discharging battery assists in maintaining DC link voltage.

Fig. 5.4 Case I schematic diagram

5.1.2 Case II: PV Charging Own Ship Battery and Supporting Ship's AC Load

This case simulates a day time scenario wherein PV power is available but there is no target ship/ battery to charge from the solar ship. This is a condition during patrolling, wherein, all sister ships are fully charged beforehand, say starting of the patrolling operation. In such a scenario, it is envisaged that the energy as harnessed from the PV panels could be utilized to cater for ship's AC load by connecting PV inverter to the DC link. The PV generation in this case also operates at the MPP, to allow the solar energy to cater for maximum load. The role of the battery bank in this case also is the same, wherein while one set is charged from the PV energy, the other charged set of battery assists in supporting the DC link voltage. In this case maintenance of the DC link voltage is essential to obtain requisite and stable voltage levels at the output of the PV inverter. The simulation study undertaken caters for a single phase AC load, thereby utilizing single phase PV inverter. Illustration of the connected circuit in this case is shown in Fig. 5.5.

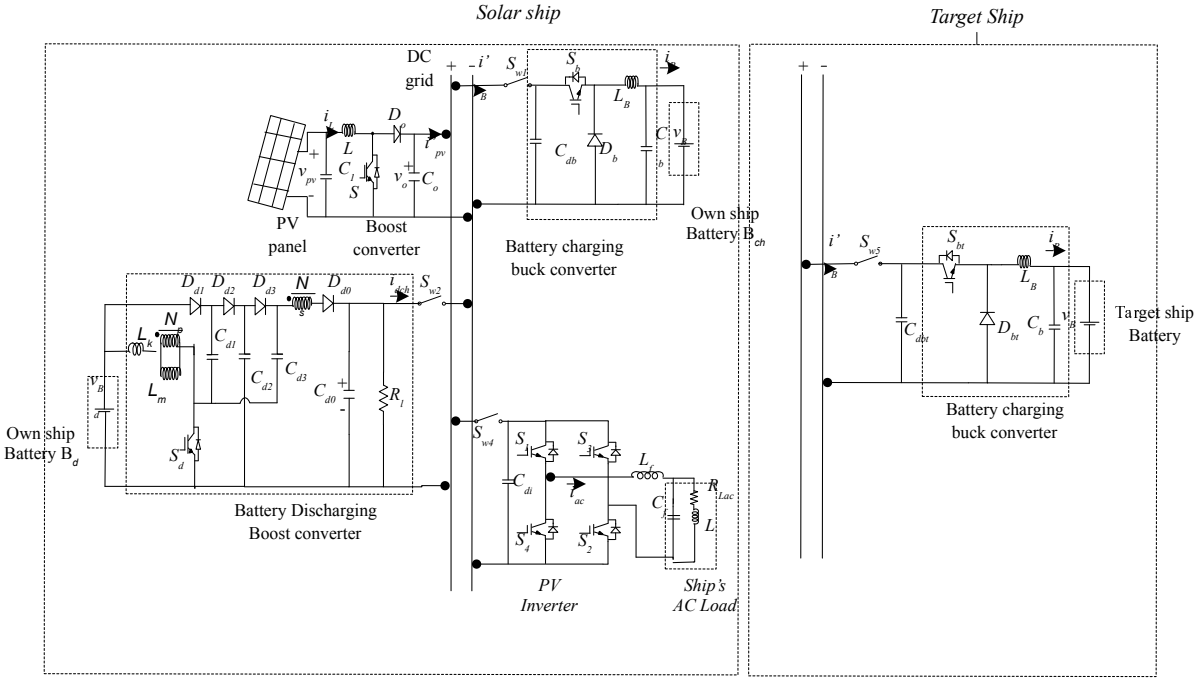

- Mode II: PV charging own ship battery and caters for ship's AC load.
- Target ship battery not charged in this case.
- Discharging battery assists in maintenance of DC link.

Fig. 5.5 Case II schematic diagram

5.1.3 Case III: Own Ship Battery Charging Target Ship Battery in Absence of PV

This case simulates a night time scenario, wherein, PV power is unavailable but there is a target ship/ battery to be charged from the solar ship. Such an operation is night UNREP and is at times required during the course of operations. In such a scenario, the charged battery from the battery bank would be utilized for transfer of energy between the solar ship and the target ship. The evolution requires disconnection of the charging circuit from the DC link to prevent it from feeding on the own ship battery. Requisite control of the relays is exercised in this scenario to ensure complete transfer of energy from the own ship battery to the target ship battery. The focus in this case is to maintain a constant charging current for the target battery, which is obtained by requisite loading of the boost converter. Illustration of the connected circuit in this case is shown in Fig. 5.6.

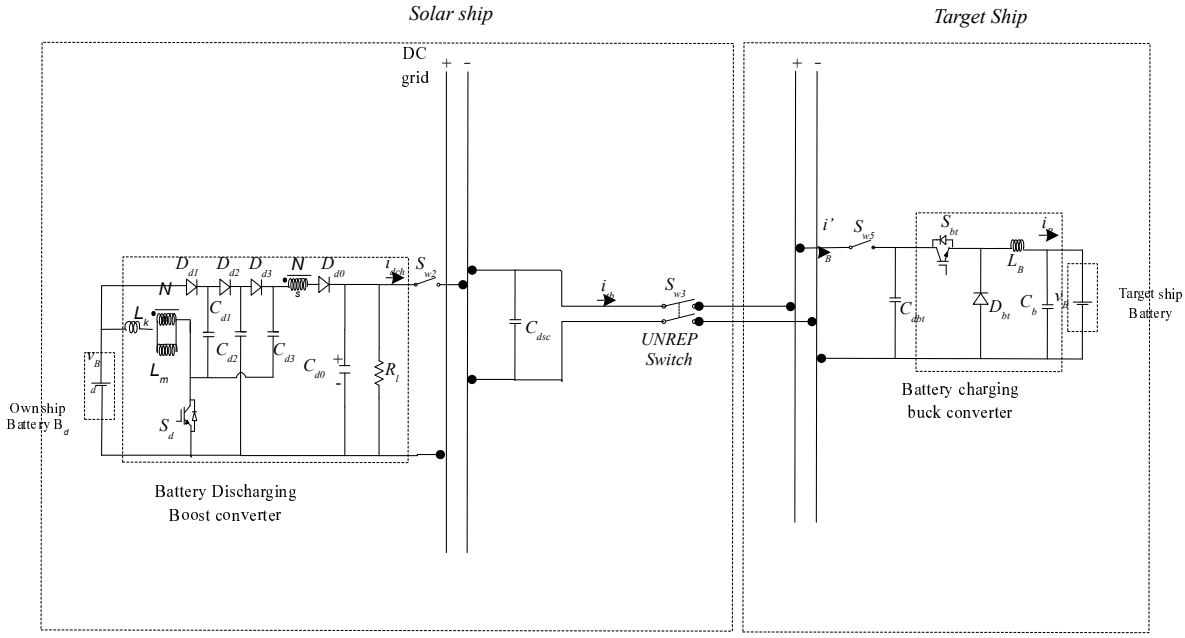

- Mode III: Own ship battery charging target battery in absence of PV.
- Charging circuit disconnected in this case.
- UNREP switch in ON position.
- AC load disconnected.

Fig. 5.6 Case III schematic diagram

5.1.4 Case IV: Own Ship Battery Supporting AC Load

This case simulates a night time scenario, wherein, PV power is unavailable and there is no target ship/battery for charging. In such a case, the stored energy from the PV panels during the day time can be utilized to power the ship's AC loads. This situation can be thought of as a ship at anchorage and the ship command desires to switch of ship's generators for maintenance or for reduction of fuel consumption. In this case also, it is required that the battery charging circuit is disconnected from the DC link and requisite DC link voltage is maintained by requisite loading of the boost converter of the battery discharging circuit. The voltage at the input of the PV inverter is required to be stable, thereby the need to maintain stable DC link voltage. Illustration of the connected circuit in this case is shown in Fig. 5.7.

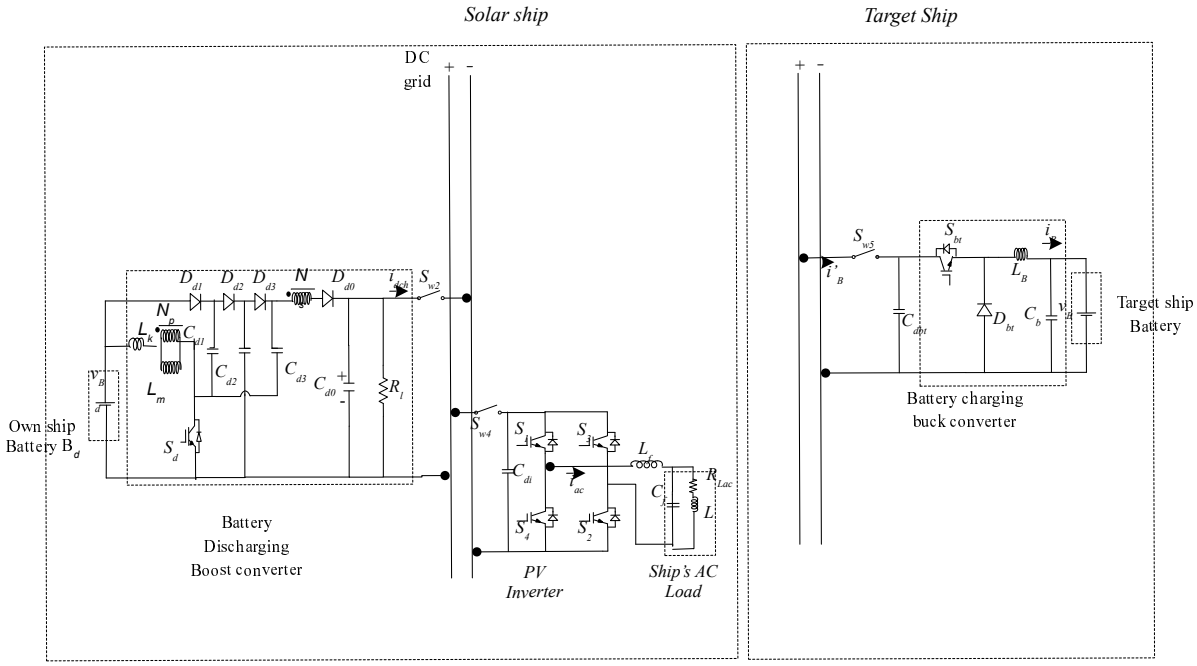

- Mode IV: Own ship battery and caters for ship's AC load in absence of PV.
- Target ship battery not charged in this case.
- Charging battery circuit disconnected.

Fig. 5.7 Case IV schematic diagram

5.2 Simulation Results

All of the above described cases were implemented in Matlab/Simulink environment sequentially and the results were obtained for each case. Further, the results were

analyzed under the purview of limitations of the study. In order to implement the discussed methodology, the solar irradiation is considered constant at 1000 W/m^2. Also, while the voltage requirement at the AC load is catered by controlling DC link voltage, the current requirement is assumed to be sufficient. However, it is understood that the current value can be increased by adjusting the solar panel configuration and increasing the battery capacity. Further, it is also assumed that a charging current control similar to own ship battery is existent and is internal to the target ship and thereby not considered as part of this study. The simulation results for each case are presented subsequently in this chapter.

5.2.1 Case I: PV Charging Target Ship Battery and Own Ship Battery

Implementation of this case, wherein, the PV system has to charge own ship battery and support the UNREP evolution to charge the target ship battery requires the PV panel to operate at the Maximum Power Point, so as to deliver maximum possible power for energy storage. This is achieved by implementation of P & O MPPT algorithm using boost converter. The use of boost converter was advocated over other converters owing to the requirement to achieve a large value of DC link voltage so as to be in line for utilization with PV inverter in case II. The output power of the boost converter illustrating the MPP operation of the system is shown in Fig. 5.8. Since, the simulation is carried out using 4 kW PV panel; the operation at MPP is validated.

The DC link voltage obtained during the course of the simulation is shown in Fig. 5.9. It is observed that the set up achieves constant DC link voltage for its connection to DC load in this case. Further, in this case the DC link is connected to two DC loads in the form of own ship battery and the target ship battery. Both the batteries are required to be charged with regulated charging current. The charging current control is implemented for the own ship battery with the assumption that similar control would be implemented at the target ship. Fig. 5.10 illustrates charging current for the target ship battery and Fig. 5.11 brings out the controlled charging current for the own ship battery as obtained from the simulation. The corresponding increase in SOC for both the target battery and own ship battery, establishing the charging operation is illustrated in Figs. 5.12 and 5.13 .

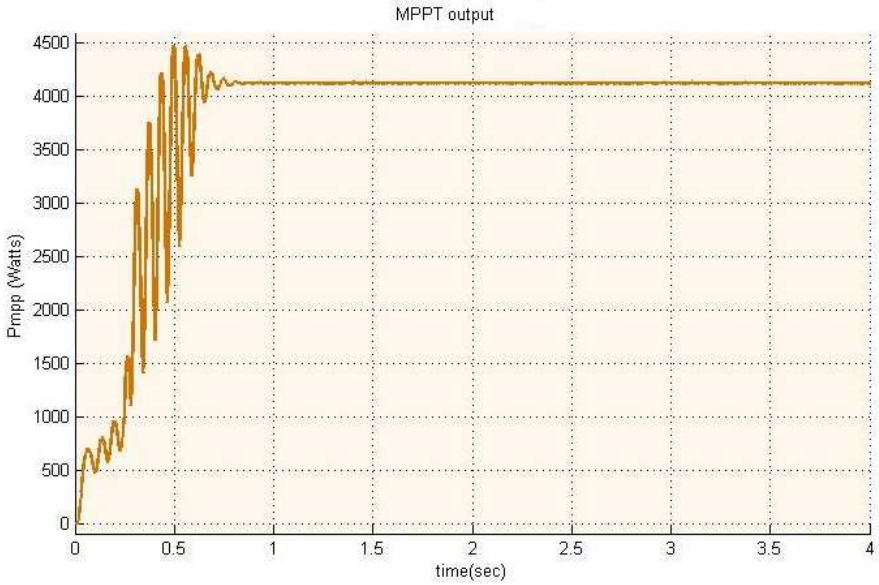

Fig. 5.8 Boost converter output depicting MPPT implementation

Fig. 5.9 Case I DC link voltage

5.2.2 Case II: PV Charging Own Ship Battery and Supporting Ship's AC Load

Implementation of this case, wherein, the PV system has to charge own ship battery and support the ship's AC load requires the PV panel to operate at the Maximum Power Point, so as to deliver maximum possible power for energy storage. Besides,

Fig. 5.10 Case I target ship battery charging current

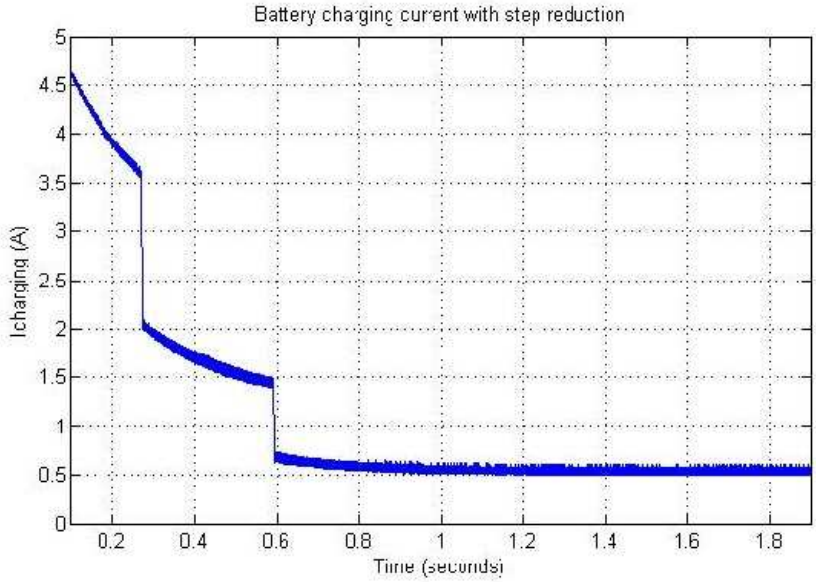

Fig. 5.11 Case I own ship battery charging current

the requirement of maintaining a stable DC link voltage is essential to achieve desired output of the PV inverter to support AC load. The output power of the boost converter illustrating the MPP operation of the PV system is shown in Fig. 5.14. The DC link voltage obtained during the course of the simulation is shown in Fig. 5.15.

The DC link in this case is connected to both the DC load in the form of own ship battery and AC load. Therefore, output voltage and current as obtained at output of the PV inverter are shown in Figs 5.16 and 5.17. The result values are in line for supporting

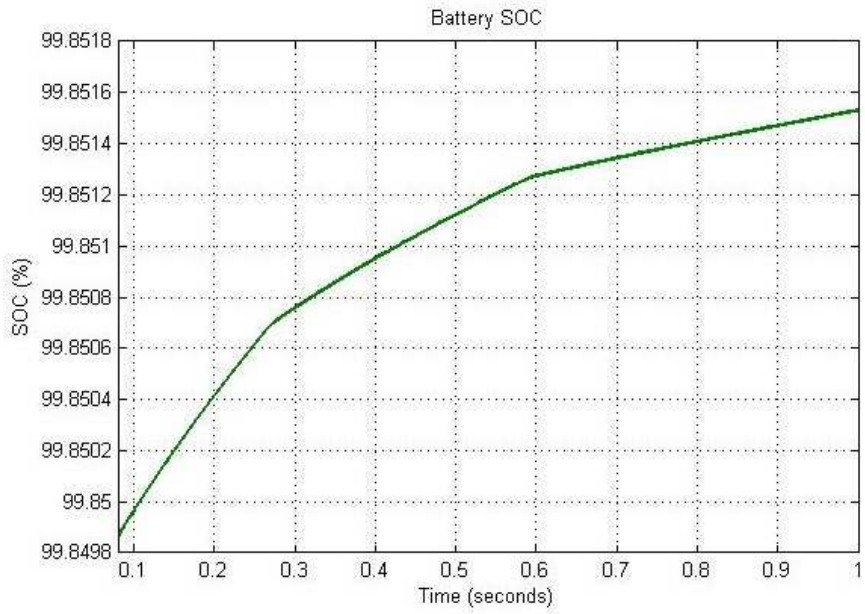

Fig. 5.12 Own ship battery SOC

Fig. 5.13 Target ship battery SOC

an AC load at 230 V, 50 Hz ac. However, current values obtained in the simulation are less, which can be increased with increase in current output rating of the solar panel by employing parallel connection of the solar panels; thereby further increasing power output of the solar panel. On the other hand, charging current for the own ship battery and the corresponding SOC is shown in Figs. 5.18 and 5.19. The charged battery complimentary to the charging battery assists in maintenance of the DC link voltage and is discharged in the process which is shown in Fig. 5.20.

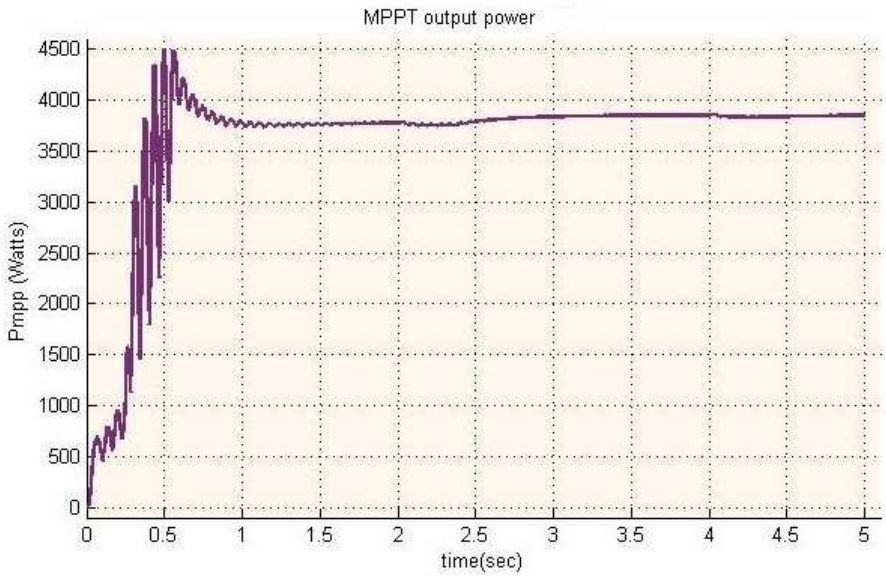

Fig. 5.14 Case II: Boost converter output depicting MPPT implementation

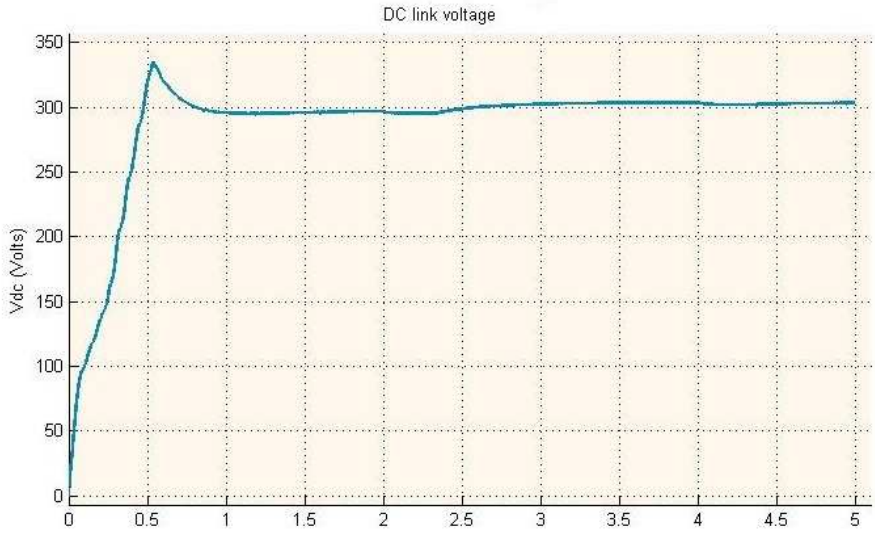

Fig. 5.15 Case II DC link voltage

5.2.3 Case III: Own Ship Battery Charging Target Ship Battery in Absence of PV

This case simulates a night UNREP scenario, wherein, PV power is unavailable but there is a target ship/ battery to be charged from the solar ship. In this case, the requirement is to maintain a constant charging current for the target ship battery. The charged battery from the solar ship, which has been charged in the day time operation, is now utilized to transfer the stored energy to the target ship. The target battery charging current as obtained in the simulation is shown in the Fig. 5.21. Also, Fig. 5.22 illustrates

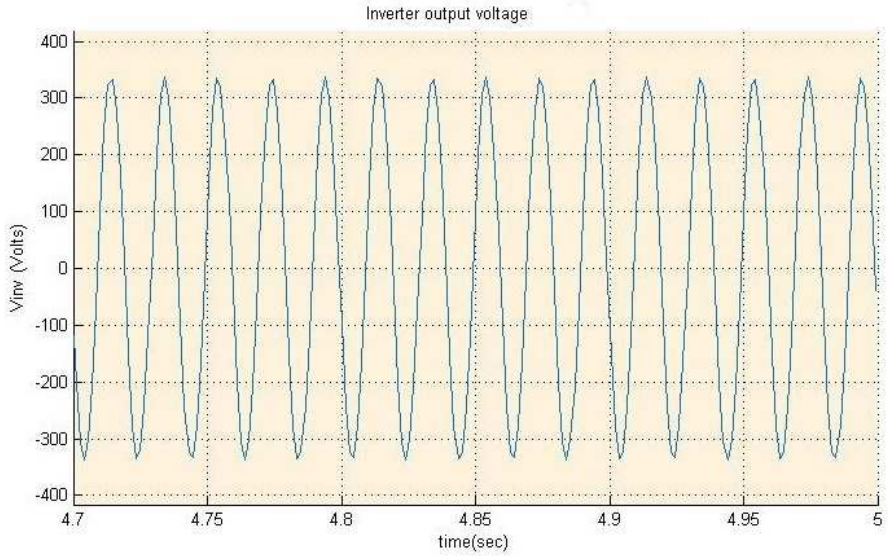

Fig. 5.16 Case II PV inverter output voltage

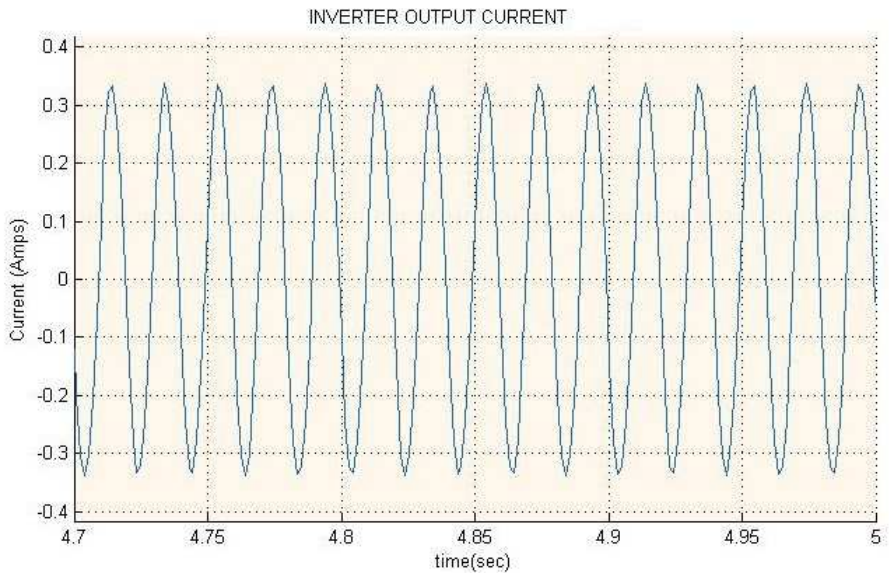

Fig. 5.17 Case II PV inverter output current

the SOC condition of both the target ship battery and own ship battery, establishing the transfer of energy from the solar ship to the target ship.

5.2.4 Case IV: Own Ship Battery Supporting AC Load

This case simulates an anchorage scenario, wherein, PV power is unavailable and there is no target ship/battery for charging. In such a case, the stored energy from the PV panels during the day time can be utilized to power the ship's AC loads. In such

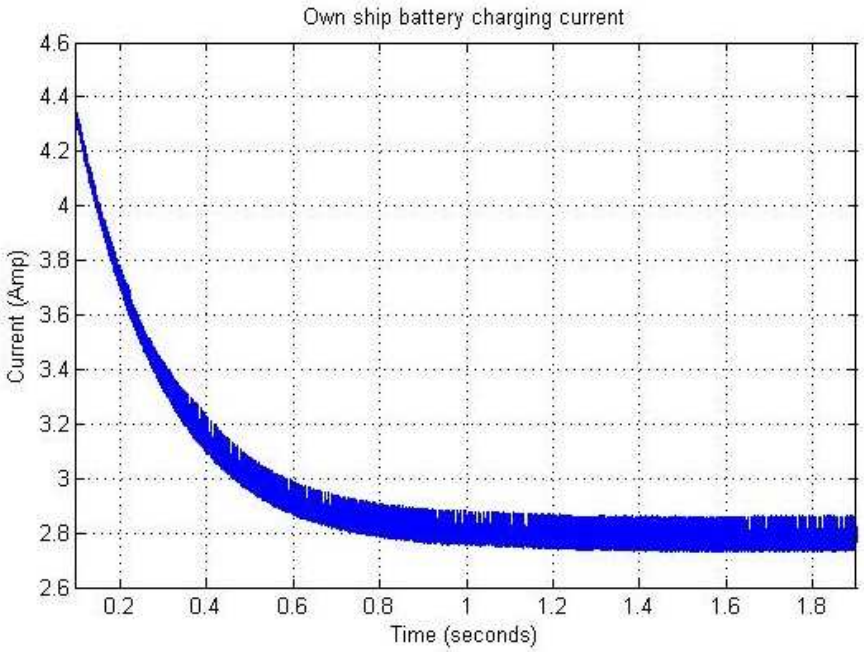

Fig. 5.18 Case II own ship battery charging current

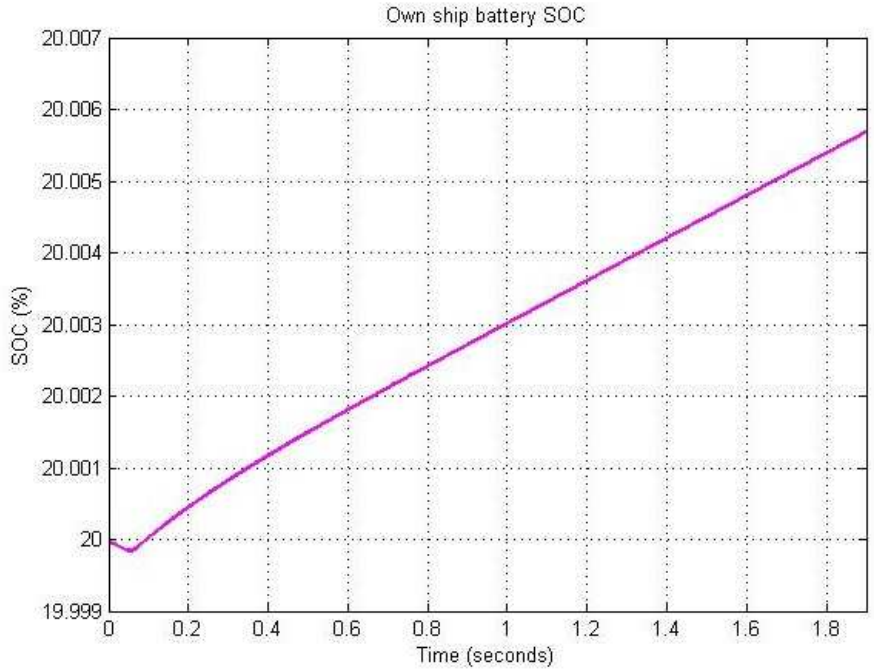

Fig. 5.19 Case II own ship battery SOC

a situation, it is essential to maintain the DC link voltage to a level required for PV inverter to support AC loads at its output. The charged battery now is connected to the PV inverter and is required to transfer the stored energy to cater for AC load. SOC of the battery showing its discharge and DC link voltage are shown in Figs. 5.23 and 5.24. Also, output voltage and current waveforms as obtained at the output of PV inverter are

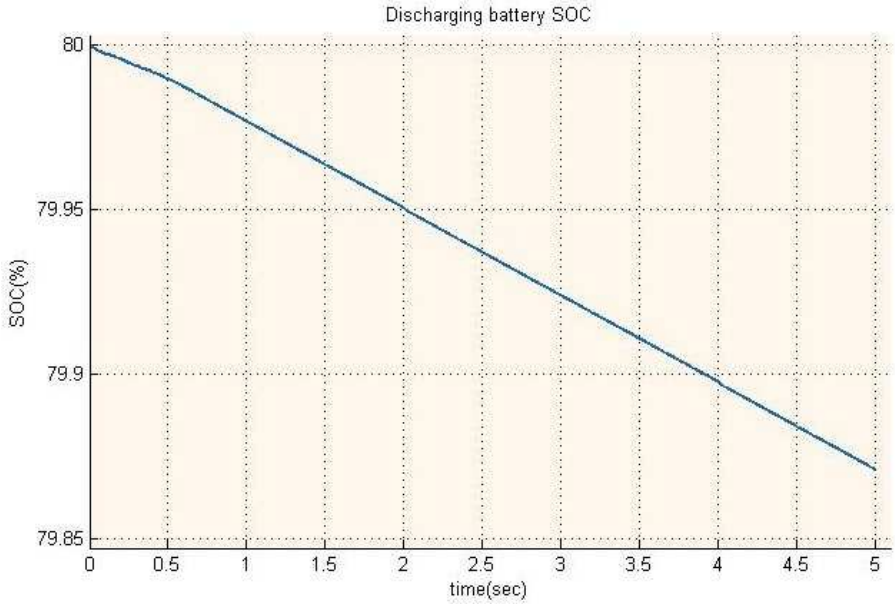

Fig. 5.20 Case II own ship discharging battery SOC

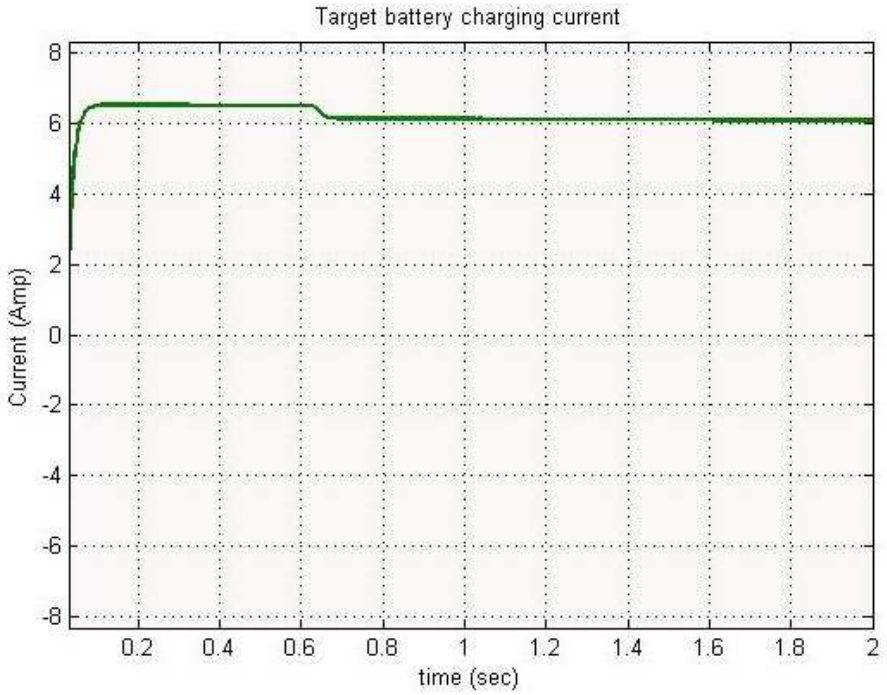

Fig. 5.21 Case III target ship battery charging current

shown in the Figs. 5.25 and 5.26.

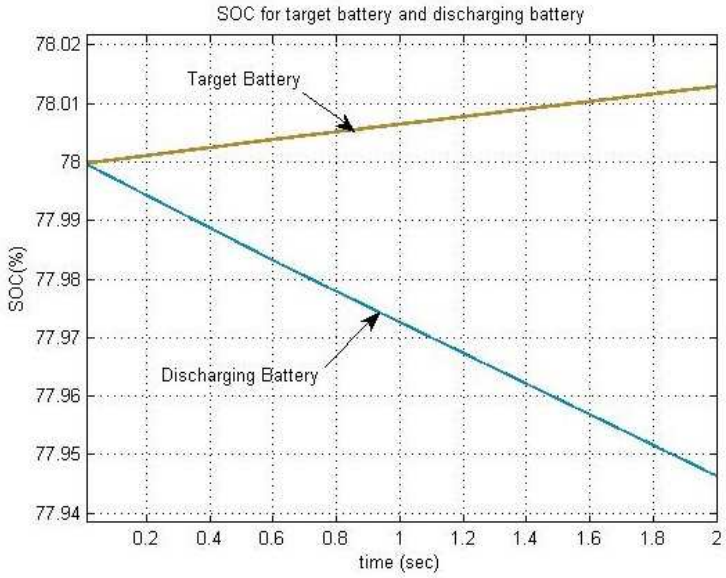

Fig. 5.22 Case III SOC for target ship battery and discharging own ship battery

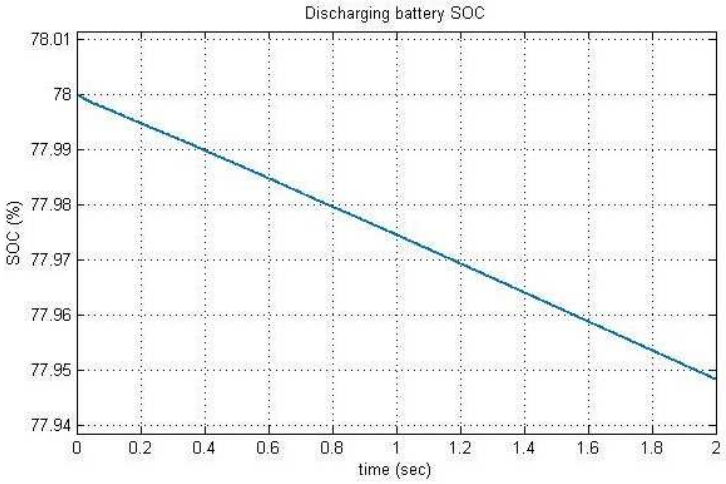

Fig. 5.23 Case IV SOC for own ship discharging battery

5.3 Conclusion

The chapter discusses different cases of operation elaborately, charting out the circuitry involved in each of the cases. Relevant block diagrams are also provided to illustrate each of the modes. Further, results obtained from the simulation study in Matlab/Simulink environment is provided in the chapter to verify the proposed ideas of the study.

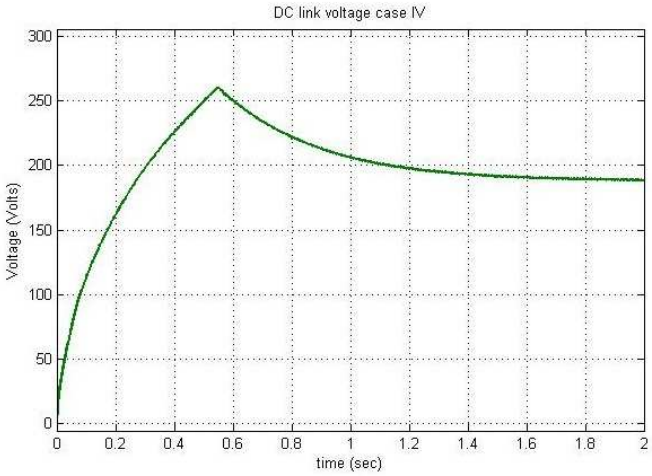

Fig. 5.24 Case IV DC link voltage

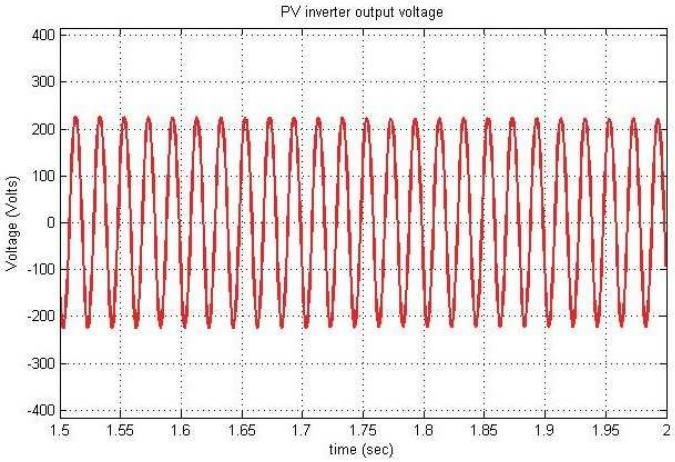

Fig. 5.25 Case IV PV inverter output voltage

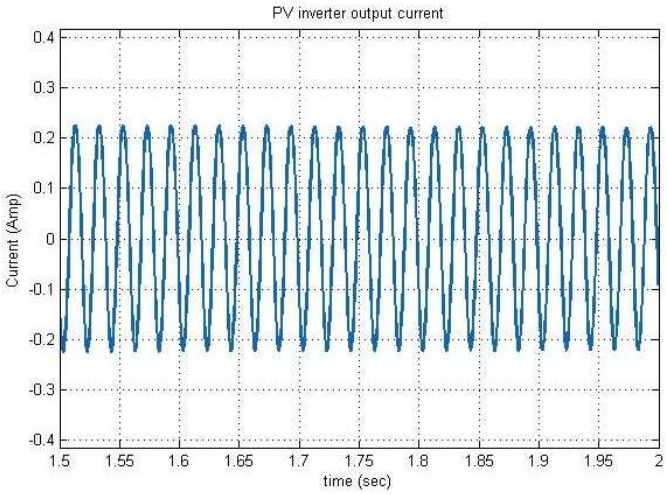

Fig. 5.26 Case IV PV inverter output current

Chapter 6

CONCLUSION AND FUTURE SCOPE

6.1 Summary

This report suggests a methodology for electrical replenishment at sea for naval ships, utilizing the UNREP (Underway replenishment at sea) procedure. The study envisages proposing a method to include the use of green fuel for operational purposes in the naval scenario. The study undertaken was based on data for the naval warships; however, the procedure can be generalized for all classes of ships, including the merchant vessels utilized for the commercial purposes.

The study was based on the use of solar energy after establishing its suitability for the naval scenario and thereby undertaking a feasibility study for its fitment on the existing ships of the navy. However, due to presence of a large number of tactical and operational machinery on the upper deck of the existing ships, the study proposed the design of a solar ship to meet the load requirements. The sizing of such hypothesized solar ship was also undertaken as part of the feasibility study and results produced as part of this study.

Further, for validation of the proposed methodology, a simulation study based on the scaled down version of the sample data was undertaken in Matlab/Simulink environment. The proposed circuitry included the use of boost converter to harness the energy from solar panels utilizing the MPPT algorithm. Further, the topology included complimentary set of batteries to maintain constant DC link voltage, wherein, a charged set of batteries assist in DC link voltage maintenance at all times. Besides, charging and discharging circuitry as utilized for the batteries has been discussed at length as part of this report. The study included testing of the circuitry for four cases, i.e.,

- PV charging target ship battery and own ship battery.
- PV charging own ship battery and supporting ship's AC load.
- Own ship battery charging target ship battery in absence of PV.
- Own ship battery supporting AC load.

The relevant results for each of the operational cases were brought out as part of the study. Based on the observed results it was validated that the proposed methodology can be utilized for implementation on naval ships, thereby achieving two headed advantage of reducing air and water pollution due to naval ships owing to the extensive dependence on diesel. Secondly, enhancing the longevity of naval ships at sea for critical patrolling operations. This owes to the fact that availability of an alternate source of energy would allow ships to stay at sea for a longer time for the same amount of fuel usage.

6.2 Future Scope

Future scope of work for the present study as foreseen are

- The study utilizes complimentary batteries for stabilization of the DC link voltage. A control algorithm to allow dynamic operation of a single battery set for undertaking charge or discharge operation as required can be formulated.
- Validation of the proposed methodology by developing a lab prototype model.
- The study can be further undertaken with use of hybrid energy storage system such as super capacitors in combination with batteries to cater for pulse loads.
- Redox flow batteries can be modeled and analyzed for the proposed set up owing to its less maintainability.

Bibliography

[1] Erik Kyrkjebø, Kristin Y Pettersen, Michiel Wondergem, and Henk Nijmeijer. Output synchronization control of ship replenishment operations: Theory and experiments. *Control Engineering Practice*, 15(6):741–755, 2007.

[2] H. Bahrami, H. Iman-Eini, B. Kazemi, and A. Taheri. Modified step-up boost converter with coupled-inductor and super-lift techniques. *IET Power Electronics*, 8(6):898–905, 2015.

[3] Surekha Dudhani, AK Sinha, and SS Inamdar. Assessment of small hydropower potential using remote sensing data for sustainable development in india. *Energy Policy*, 34(17):3195–3205, 2006.

[4] Y. Qiu, C. Yuan, and Y. Sun. Review on the application and research progress of photovoltaics-ship power system. In *2015 International Conference on Transportation Information and Safety (ICTIS)*, pages 523–527, June 2015.

[5] Stanley W Angrist. Direct energy conversion. 1976.

[6] Huan-Liang Tsai, Ci-Siang Tu, Yi-Jie Su, et al. Development of generalized photovoltaic model using matlab/simulink. In *Proceedings of the world congress on Engineering and computer science*, volume 2008, pages 1–6. San Francisco, USA, 2008.

[7] Chihchiang Hua and Chihming Shen. Study of maximum power tracking techniques and control of dc/dc converters for photovoltaic power system. In *PESC 98 Record. 29th Annual IEEE Power Electronics Specialists Conference (Cat. No.98CH36196)*, volume 1, pages 86–93 vol.1, May 1998.

[8] M. Veerachary, T. Senjyu, and K. Uezato. Voltage-based maximum power point tracking control of pv system. *IEEE Transactions on Aerospace and Electronic Systems*, 38(1):262–270, 2002.

[9] Trishan Esram and Patrick L Chapman. Comparison of photovoltaic array maximum power point tracking techniques. *IEEE Transactions on energy conversion*, 22(2):439–449, 2007.

[10] O Wasynezuk. Dynamic behavior of a class of photovoltaic power systems. *IEEE transactions on power apparatus and systems*, (9):3031–3037, 1983.

[11] GW Hart, HM Branz, and CH Cox. Experimental tests of open-loop maximum-power-point tracking techniques for photovoltaic arrays. *Solar cells*, 13(2):185–195, 1984.

[12] Bernard Bekker and HJ Beukes. Finding an optimal pv panel maximum power point tracking method. In *AFRICON, 2004. 7th AFRICON Conference in Africa*, volume 2, pages 1125–1129. IEEE, 2004.

[13] Toshihiko Noguchi, Shigenori Togashi, and Ryo Nakamoto. Short-current pulse-based maximum-power-point tracking method for multiple photovoltaic-and-converter module system. *IEEE Transactions on Industrial Electronics*, 49(1):217–223, 2002.

[14] Subbaraya Yuvarajan and Shanguang Xu. Photo-voltaic power converter with a simple maximum-power-point-tracker. In *Circuits and Systems, 2003. ISCAS'03. Proceedings of the 2003 International Symposium on*, volume 3, pages III–III. IEEE, 2003.

[15] Nopporn Patcharaprakiti and Suttichai Premrudeepreechacharn. Maximum power point tracking using adaptive fuzzy logic control for grid-connected photovoltaic system. In *Power Engineering Society Winter Meeting, 2002. IEEE*, volume 1, pages 372–377. IEEE, 2002.

[16] Chao Zhang and Dean Zhao. Mppt with asymmetric fuzzy control for photovoltaic system. In *Industrial Electronics and Applications, 2009. ICIEA 2009. 4th IEEE Conference on*, pages 2180–2183. IEEE, 2009.

[17] Jiyong Li and Honghua Wang. Maximum power point tracking of photovoltaic generation based on the fuzzy control method. In *Sustainable Power Generation and Supply, 2009. SUPERGEN'09. International Conference on*, pages 1–6. IEEE, 2009.

[18] Takashi Hiyama, Shinichi Kouzuma, and Tomofumi Imakubo. Identification of optimal operating point of pv modules using neural network for real time maximum power tracking control. *IEEE Transactions on Energy Conversion*, 10(2):360–367, 1995.

[19] Kyoungsoo Ro and Saifur Rahman. Two-loop controller for maximizing performance of a grid-connected photovoltaic-fuel cell hybrid power plant. *IEEE Transactions on Energy Conversion*, 13(3):276–281, 1998.

[20] JM Enrique, E Duran, M Sidrach-de Cardona, and JM Andujar. Theoretical assessment of the maximum power point tracking efficiency of photovoltaic facilities with different converter topologies. *Solar Energy*, 81(1):31–38, 2007.

[21] Xin Qiu, Tu A Nguyen, Joe D Guggenberger, Mariesa L Crow, and Andrew Curtis Elmore. A field validated model of a vanadium redox flow battery for microgrids. *IEEE Transactions on Smart Grid*, 5(4):1592–1601, 2014.

[22] J Chahwan, C Abbey, and G Joos. Vrb modelling for the study of output terminal voltages, internal losses and performance. In *Electrical Power Conference, 2007. EPC 2007. IEEE Canada*, pages 387–392. IEEE, 2007.

[23] Guishi Wang, Mihai Ciobotaru, and Vassilios G Agelidis. Integration of vanadium redox battery with pv systems: Modeling and operational characteristics. In *Industrial Electronics (ISIE), 2012 IEEE International Symposium on*, pages 1598–1603. IEEE, 2012.

[24] L Barote, C Marinescu, and M Georgescu. Vrb modeling for storage in standalone wind energy systems. In *PowerTech, 2009 IEEE Bucharest*, pages 1–6. IEEE, 2009.

[25] Maria Skyllas-Kazacos and C Menictas. The vanadium redox battery for emergency back-up applications. In *Telecommunications Energy Conference, 1997. INTELEC 97., 19th International*, pages 463–471. IEEE, 1997.

[26] S. Mane, P. Kadam, G. Lahoti, F. Kazi, and N. M. Singh. Optimal load balancing strategy for hybrid energy management system in dc microgrid with pv, fuel cell and battery storage. In *2016 IEEE International Conference on Renewable Energy Research and Applications (ICRERA)*, pages 851–856, Nov 2016.

[27] H. Choi, M. Jang, M. Ciobotaru, and V. G. Agelidis. Hybrid energy storage for large pv systems using bidirectional high-gain converters. In *2016 IEEE International Conference on Industrial Technology (ICIT)*, pages 425–430, March 2016.

[28] Xiaoyu Wang and M. Yue. Capacity specification for hybrid energy storage system to accommodate fast pv fluctuations. In *2015 IEEE Power Energy Society General Meeting*, pages 1–5, July 2015.

[29] E Koutroulis and K Kalaitzakis. Novel battery charging regulation system for photovoltaic applications. *IEE Proceedings-Electric Power Applications*, 151(2):191–197, 2004.

[30] Tsutomu Yamazaki and Ken-Ichiro Muramoto. An advanced solar charging and battery discharge controller unit. *Renewable energy*, 15(1-4):606–609, 1998.

[31] Joseph R Woodworth, Michael G Thomas, John W Stevens, Steven R Harrington, James P Dunlop, and M Ramu Swamy. Evaluation of the batteries and charge controllers in small stand-alone photovoltaic systems. In *Photovoltaic Energy Conversion, 1994., Conference Record of the Twenty Fourth. IEEE Photovoltaic Specialists Conference-1994, 1994 IEEE First World Conference on*, volume 1, pages 933–945. IEEE, 1994.

[32] Shane Duryea, Syed Islam, and William Lawrance. A battery management system for stand alone photovoltaic energy systems. In *Industry Applications Conference, 1999. Thirty-Fourth IAS Annual Meeting. Conference Record of the 1999 IEEE*, volume 4, pages 2649–2654. IEEE, 1999.

[33] Athimulam Kalirasu and Sekar Subharensu Dash. Simulation of closed loop controlled boost converter for solar installation. *Serbian Journal of Electrical Engineering*, 7(1):121–130, 2010.

[34] W. Li, J. Xiao, J. Wu, J. Liu, and X. He. Application summarization of coupled inductors in dc/dc converters. In *2009 Twenty-Fourth Annual IEEE Applied Power Electronics Conference and Exposition*, pages 1487–1491, Feb 2009.

[35] B Santhosh Kumar and M Ramalingaraju. Stand-alone pv hybrid system for residential applications. In *Electrical, Electronics, and Optimization Techniques (ICEEOT), International Conference on*, pages 2035–2040. IEEE, 2016.

[36] Luiz Henrique SC Barreto, Paulo Peixoto Praca, Demercil S Oliveira, and Ranoyca NAL Silva. High-voltage gain boost converter based on three-state commutation cell for battery charging using pv panels in a single conversion stage. *IEEE Transactions on Power Electronics*, 29(1):150–158, 2014.

[37] E-H Kim and B-H Kwon. High step-up resonant push–pull converter with high efficiency. *IET Power Electronics*, 2(1):79–89, 2009.

[38] Y Zhao, W Li, Y Deng, and X He. High step-up boost converter with passive lossless clamp circuit for non-isolated high step-up applications. *IET power electronics*, 4(8):851–859, 2011.

[39] Rong-Jong Wai, Chung-You Lin, Rou-Yong Duan, and Yung-Ruei Chang. High-efficiency dc-dc converter with high voltage gain and reduced switch stress. *IEEE Transactions on Industrial Electronics*, 54(1):354–364, 2007.

[40] Wuhua Li, Yi Zhao, Yan Deng, and Xiangning He. Interleaved converter with voltage multiplier cell for high step-up and high-efficiency conversion. *IEEE transactions on power electronics*, 25(9):2397–2408, 2010.

[41] Sergio Ignacio Serna-Garcés, Daniel Gonzalez Montoya, and Carlos Andres Ramos-Paja. Sliding-mode control of a charger/discharger dc/dc converter for dc-bus regulation in renewable power systems. *Energies*, 9(4):245, 2016.

[42] Emil A Jimenez Brea, Eduardo I Ortiz-Rivera, Andres Salazar-Llinas, and Jesus Gonzalez-Llorente. Simple photovoltaic solar cell dynamic sliding mode controlled maximum power point tracker for battery charging applications. In *Applied Power Electronics Conference and Exposition (APEC), 2010 Twenty-Fifth Annual IEEE*, pages 666–671. IEEE, 2010.

[43] M Subashini and M Ramaswamy. A novel design of charge controller for a standalone solar photovoltaic system. In *Electrical Energy Systems (ICEES), 2016 3rd International Conference on*, pages 237–243. IEEE, 2016.

[44] Merahi Reda and Chenni Rachid. Control strategy for dc bus voltage regulation in photovoltaic system with battery energy.